Journal of Proteomics xxx (2016) xxx–xxx

Contents lists available at ScienceDirect

Journal of Proteomics

journal homepage: www.elsevier.com/locate/jprot

Modifications to the composition of the hyphal outer layer of *Aspergillus fumigatus* modulates HUVEC proteins related to inflammatory and stress responses

Gabriela Westerlund Peixoto Neves [a], Nathália de Andrade Curty [a], Paula Helena Kubitschek-Barreira [a], Thierry Fontaine [c], Gustavo Henrique Martins Ferreira Souza [b], Marcel Lyra Cunha [a], Gustavo H. Goldman [d], Anne Beauvais [c], Jean-Paul Latgé [c], Leila M. Lopes-Bezerra [a,*]

[a] *Laboratory of Cellular Mycology and Proteomics, Universidade do Estado do Rio de Janeiro, Campus Maracanã, Pavilhão Haroldo Lisboa da Cunha sl 501D, CEP: 20550-013, Rio de Janeiro, RJ, Brazil*
[b] *MS Applications Research and Development Laboratory, Waters Corporation, São Paulo, Brazil*
[c] *Unité des Aspergillus, Institut Pasteur, 25 rue du Docteur Roux, 75724, Paris Cedex 15, France*
[d] *Universidade de São Paulo, Faculdade de Ciências Farmacêuticas de Ribeirão Preto, Departamento de Ciências Farmacêuticas, Av. do Cafe S/N, Monte Alegre, CEP:14040-903, Ribeirao Preto, SP, Brazil*

ARTICLE INFO

Article history:
Received 1 February 2016
Received in revised form 20 April 2016
Accepted 7 June 2016
Available online xxxx

Keywords:
HUVEC
Aspergillus fumigatus
Inflammatory response
Δugm1 mutant
Galactosaminogalactan

ABSTRACT

Aspergillus fumigatus, the main etiologic agent causing invasive aspergillosis, can induce an inflammatory response and a prothrombotic phenotype upon contact with human umbilical vein endothelial cells (HUVECs). However, the fungal molecules involved in this endothelial response remain unknown. *A. fumigatus* hyphae produce an extracellular matrix composed of galactomannan, galactosaminogalactan and α-(1,3)-glucan. In this study, we investigated the consequences of *UGM1* gene deletion in *A. fumigatus*, which produces a mutant with increased galactosaminogalactan production. The Δ*ugm1* mutant exhibited an HUVEC-hyperadhesive phenotype and induced increased endothelial TNF-α secretion and tissue factor mRNA overexpression in this "semi-professional" immune host cell. Using a shotgun proteomics approach, we show that the *A. fumigatus* Δ*ugm1* strain can modulate the levels of proteins in important endothelial pathways related to the inflammatory response mediated by TNF-α and to stress response pathways. Furthermore, a purified galactosaminogalactan fraction was also able to induce TNF-α secretion and the coincident HUVEC pathways regulated by the Δ*ugm1* mutant, which overexpresses this component, as demonstrated by fluorescence microscopy. This work contributes new data regarding endothelial mechanisms in response to *A. fumigatus* infection.

Significance: Invasive aspergillosis is the main opportunistic fungal infection described in neutropenic hematologic patients. One important clinical aspect of this invasive fungal infection is vascular thrombosis, which could be related, at least in part, to the activation of endothelial cells, as shown in previous reports from our group. It is known that direct contact between the *A. fumigatus* hyphal cell wall and the HUVEC cell surface is

Abbreviations: AiP, programed cell death 6-interacting protein; AKT, protein kinase B; ASK1, mitogen-activated protein kinase 5; BAD, BLC2-associated agonist of cell death; BAX, BCL2-associated X protein; CD-142, tissue factor; cFOS, FBJ Murine osteosarcoma viral oncogene homolog; CID, collision-induced dissociation; cJUN, Jun Proto-Oncogene; CRAF, Raf 1 Proto-oncogene Serine/Threonine Kinase; DAG, diacylglycerol; ECM, extracellular matrix; EIF2, eukaryotic initiation factor 2; ELISA, enzyme-Linked Immunosorbent Assay; ELK1, member of ETS Oncogene family; ERK 1/2, mitogen-activated protein kinases ERK ½; FDR, false discovery rate; FWHM, full width at half maximum; FOX01, fork head box 01; Gal*f*, galactofuranose; GalNAc, uracil diphosphate-n acetylgalactosamine; Gal*p*, galactopyranose; GAPDH, glyceraldehyde 3-phosphate dehydrogenase; GFAP, glial Fibrillary Acid Protein; GAG, galactosaminogalactan; Glu-Fib, [Glu[1]]-Fibrinopeptide B human; GO, gene ontology; GRB2, growth factor receptor-binding protein 2; HDMS, high-definition mass spectrometry; HDMS^E, ion mobility multiplex low and high-collision energy acquisition; HMGB1, high mobility group box 1; HPF, high-power field; Hsp, heat shock proteins; HUVEC, human umbilical vein endothelial cells; IAA, iodoacetamide; IAP, inhibitors of apoptosis proteins; IgG, immunoglobulin G; I-kappaB, inhibitor of *kappa B*; IL-6, interleukin 6; IL-8, interleukin 8; ILK, integrin like kinase; IPA, ingenuity pathway analysis software; IRF3, interferon transcription factor 3; JNK, c-Jun N-terminal Protein Kinase; kDa, KiloDalton; LBL, Lbl proto-oncogene/E3 ubiquitin protein ligase; LKB1, serine/Threonine Kinase 11; LPS, lipopolysaccharide; M-199, medium 199; MAPK, mitogen-activated protein kinase; MEK1/2, mitogen-activated Protein Kinases MEK1/2; MS^E, multiplex low and high-collision energy acquisition; mTOR, serine/threonine-protein kinase mTOR; MyD88, myeloid differentiation primary response 88; NAF, sodium fluoride; NF-kappaB, factor nuclear *kappa B*; NF-κB, factor nuclear kappa B; *oa*-TOF, orthogonal acceleration time of flight; P13K-1, phosphatidylinositol 3 kinase; P27KIP1, cyclin-dependent kinase inhibitor 1B; P73, tumor protein P73; p90RSK, ribosomal protein S6 kinase 90 kDa polypeptide 1; PI3, phosphatidylinositol 3; PKC, protein kinase C; PLC, phospholipase C; PRAS40, AKT1 substrate 1; pyrG, CTP synthase; RF, radiofrequency; RNA, ribonucleic acid; RP, reverse phase; RTK, receptor tyrosine kinase; RT-PCR, real-time polymerase chain reaction; SBL, SBL proto-oncogene or E3 ubiquitin protein ligase; SEM, scanning electron microscopy; SNCα, synuclein α; SRC, SRC proto-oncogene; SRPK2, SRSF protein kinase 2; STRADA, STE20-related kinase adaptor α; TAU, microtubule-associated protein TAU; TFG, protein TFG; Th1, T helper type 1 cells; Th2, T helper type 2 cells; TLR, toll-like receptor; TLR4, toll-like receptor 4; TNF, tumor necrosis factor; TNFR1, tumor necrosis factor receptor superfamily member 1A; TNF-α, tumor necrosis factor-α; TRAF2, tumor necrosis factor receptor-associated factor 2; Treg, regulatory T cell; TRIF, TIR-containing adaptor inducing IFNβ; TRITC, tetramethylrhodamine; TSC, tuberous sclerosis complex protein; TUBULIN, tubulin complex; T-Wave™, travelling wave; UDP, uracil diphosphate; UPLC, ultra-performance liquid chromatography; UR, upstream regulators; VIM, vimentin; WT, wild type; YAP, yes-associated protein 1.

* Corresponding author at: Laboratory of Cellular Mycology and Proteomics, State University of Rio de Janeiro, Rua São Francisco Xavier 524 PHLC 501D, cep 20550-013, Rio de Janeiro, Brazil.
E-mail addresses: leila@uerj.br, lmlb23@globo.com (L.M. Lopes-Bezerra).

http://dx.doi.org/10.1016/j.jprot.2016.06.015
1874-3919/

necessary to induce an endothelial prothrombotic phenotype and secretion of pro-inflammatory cytokines, though the cell surface components of this angioinvasive fungus that trigger this endothelial response are unknown. The present work employs a discovery-driven proteomics approach to reveal the role of one important cell wall polysaccharide of *A. fumigatus*, galactosaminogalactan, in the HUVEC interaction and the consequent mechanisms of endothelial activation. This is the first report of the overall panel of proteins related to the HUVEC response to a specific and purified cell wall component of the angioinvasive fungus *A. fumigatus*.

1. Introduction

Aspergillus fumigatus is a known angioinvasive pathogen and the main etiologic agent of invasive aspergillosis (IA) [1,2,3,4]. The disease is initiated by inhalation of airborne conidia, which reach the alveoli of susceptible hosts, producing angioinvasive hyphae upon germination [5]. During hematogenous dissemination, hyphae can interact with the luminal face of the vascular endothelium, transpose the endothelial barrier and deeply invade organs and tissues [6,7]. As the angioinvasion process leads to thrombosis and tissue infarction, it plays a key role in the pathogenesis of invasive aspergillosis [2,3]. Upon contact with fungal hyphae, endothelial cells switch to an activated prothrombotic phenotype characterized by the expression of tissue factor (CD-142) [8] and the secretion of TNF-α and IL-8 [7,9]. This process is independent of fungal viability and occurs in a hyphal contact-dependent manner [7,8]. However, the molecular mechanisms by which this pathogen can adhere to and activate endothelial cells remain unknown.

A. fumigatus hyphae produce an extracellular matrix (ECM) in both chronic and invasive aspergillosis [10] and also during the in vitro growth of the mycelium [11]. Under both *in vivo* and *in vitro* conditions, this ECM is rich in galactose polymers, namely, galactomannan, galactosaminogalactan (GAG) and α-(1,3)-glucan [10,11]. Galactomannan, a major antigen of *A. fumigatus*, is composed of β1-5 Gal*f* oligosaccharides covalently bound to a mannan chain [11,12,13]. Galactofuranose (Gal*f*) is a five-membered galactose found exclusively in microbes, especially in pathogenic species [14]. This monosaccharide has been described as a component of the glycoproteins, lipophosphogalactomannans and sphingolipids of *A. fumigatus* [15,16,17]. Gal*f* is synthesized in *A. fumigatus* by the enzyme UDP-galactopyranose mutase, which is encoded by the *UGM1* gene and converts UDP-galactopyranose (Gal*p*) to UDP-galactofuranose [18].

In contrast, GAG is a heterogeneous polymer composed of α1-4-linked Gal*p* and α1-4-linked N-acetylgalactosamine [19]. Therefore, the mutant Δ*ugm1*, resulting from deletion of the *UGM1* gene, displays an altered galactomannan free of galactofuranose, (Gal*f*) a higher production of GAG as a consequence of the lack of Gal*f* and an increased content of Gal*p* [18,20]. Remarkably, this mutant has been described as hyperadhesive to epithelial cells [18], and this hyperadhesive phenotype was further shown to be related to GAG. In addition, due to its immunomodulatory properties, GAG has also been described as an important virulence factor [20,21,22].

The aim of this work was to study the biological response of human umbilical vein endothelial cells to the wild-type and the Δ*ugm1* strains of *A. fumigatus*. In this sense, we analyzed the adhesion capacity of these strains to HUVECs and the endothelial cytokine secretion profile and expression of tissue factor in response to *A. fumigatus* infection. Furthermore, shotgun proteome analysis revealed the main endothelial pathways regulated in HUVECs upon interaction with *A. fumigatus* and the purified galactosaminogalactan.

2. Materials and methods

2.1. Strains and culture conditions

The Ku80 pyrG$^+$ parental strain [23], *UGM1* mutant (Δ*ugm1*) and reconstituted strain (Δ*ugm1*::*ugm1*) [18] were plated on Petri dishes containing Sabouraud agar (Difco, Detroit, USA) and cultivated for 7 days at 37 °C. For conidial isolation, conidia were harvested by gently rinsing the plates with 0.1% Tween 80 in 50 mM phosphate-buffered saline (PBS; pH 7.4) and washing twice in PBS. A previously described protocol was used to obtain a homogenous suspension of germlings [8]. The suspension was sonicated for three cycles of 10 s each using a Vibra Cell (Sonics, Newtown, USA). For experiments using killed organisms, germlings were incubated overnight at 4 °C in 0.02% thimerosal in PBS.

A. fumigatus conidia and germlings were counted using a hemocytometer. The cells were adjusted to the desired concentration in supplemented tissue culture medium (M-199 medium containing 2mM L-glutamine, penicillin, and streptomycin, and supplemented with 10% fetal bovine serum and 10% bovine calf serum) prior to use in the interaction experiments.

The purified urea-soluble fraction of galactosaminogalactan (GAG) was obtained as previously described [19]. Cellulose was obtained from Sigma-Aldrich (Missouri, USA).

2.2. Human vein endothelial cell (HUVEC) culture

HUVECs were obtained by treatment of umbilical veins with a 0.1% collagenase IV (Sigma) solution, as previously described [24]. Primary cells were seeded into 25-cm^2 cell culture flasks coated with porcine skin gelatin and grown at 37 °C in a humidified 5% CO_2 atmosphere in supplemented tissue culture medium (M-199, GIBCO) until reaching confluence. In this study, primary cultures were used after one (P1) or two subcultures (P2) obtained by treatment of the confluent cells with 0.025% (*v*/v) trypsin and 0.02% (*v*/v) EDTA solution in PBS. This study was approved by the Research Ethics Committee of the Municipal Health Secretary and Civil Defense of Rio de Janeiro (CEP SMSDC-RJ), protocol no196/09. A total of 18 volunteers participated in this study.

2.3. Endocytosis and adhesion assay

The number of *A. fumigatus* germlings internalized by and adhered to endothelial cells was determined as previously described [8]. Briefly, endothelial cells grown on fibronectin-coated glass coverslips in 24-well cell culture plates were infected with 6x10^4 *A. fumigatus* germlings in supplemented tissue culture medium for 45 min. A differential immunofluorescence assay was then performed.

2.4. Endothelial cell viability following fungal infection

The viability of endothelial cells exposed to *A. fumigatus* germlings and GAG of all genotypes was determined using the MTT assay [25]. Briefly, HUVECs grown to confluence in 24-well tissue culture plates were incubated for 16 h at 37 °C in 5% CO_2 with 2x10^5 *A. fumigatus* germlings in supplemented M-199. After interaction, three washing steps with serum-free M-199 were performed. The cell monolayers were incubated with MTT at 1 mg/mL in serum-free M-199 for 2 h at 37 °C in 5% CO_2. The medium containing MTT was then removed, 250 μL of isopropanol was added per well for 5 min, and 100 μl of the solution was transferred to microtiter plates. The absorbance was determined at 595 nm using a microplate reader. Three independent experiments were performed in triplicate wells.

Please cite this article as: G.W.P. Neves, et al., Modifications to the composition of the hyphal outer layer of *Aspergillus fumigatus* modulates HUVEC proteins related to inflammatory and stress responses..., J Prot (2016), http://dx.doi.org/10.1016/j.jprot.2016.06.015

2.5. Cytokine secretion and tissue factor expression in infected HUVECs

For the cytokine secretion study, endothelial monolayers were cultivated in fibronectin-coated 24-well cell culture plates and luminally infected with thimerosal-killed germlings of *A. fumigatus* WT or the mutant strains for 4 h, 8 h or 16 h. At each time point, the conditioned medium was collected, cooled on ice, and centrifuged at 1000 ×*g* for 5 min at 4 °C to remove cell debris. The supernatants were then stored at −80 °C until use. The cytokines TNF-α, IL-6 and IL-8 were determined in the conditioned media using a Multiplex kit (Millipore, Billerica, MA) or an ELISA kit specific for each cytokine (Uscnk Life Science Inc., Houston, TX), according to the manufacturer's instructions as a positive control, the endothelial cells were incubated with LPS (1 ng/mL) from *Escherichia coli* 0111.B4 (List Biological Laboratories, Campbell, CA). The same methodology described above was used to measure these cytokines in the conditioned medium after 16 h of HUVEC incubation with GAG (1 μg/mL). Cellulose was also used as a control in this assay. All experiments were performed in duplicate, and two or three independent experiments were performed.

A real-time RT-PCR assay was used to determine tissue factor (CD-142) expression by endothelial cells grown in six-well cell culture plates coated with porcine skin gelatin. Luminal infection with germlings of *A. fumigatus* strains was performed for 16 h. The medium was aspirated, and endothelial cell RNA was extracted using an RNeasy mini kit (QIAGEN GmbH, Hilden) according to the manufacturer's instructions. RT-PCR was performed as previously described [26]. The primers and Lux™ fluorescence probes (Invitrogen) used in this work are described in Supplementary Table 1. Expression of the tissue factor gene was normalized to GAPDH, and the results are expressed as the increase in expression relative to that observed in uninfected endothelial cells. The experiment was repeated four times with experimental duplicates. In all experiments, an effector:target ratio of 2:1 was used.

2.6. Statistical analysis of cellular biology data

Differences in endothelial cell responses to *A. fumigatus* strains and GAG were compared using analysis of variance followed by a Tukey-Kramer post-test or unpaired *t*-test. For datasets for which a normal distribution could not be assumed, the analysis was performed using the non-parametric Mann–Whitney *U* test. Differences between data were considered significant when $p < 0.05$.

2.7. Experimental design and statistical rationale for proteomics

2.7.1. HUVEC interaction with A. fumigatus for proteomics

For the proteomics experiments, HUVEC monolayers were infected with thimerosal-killed germlings of *A. fumigatus* WT and the Δ*ugm1* strain, as described above, at a 5:1 ratio (five organisms per endothelial cell). Alternatively, HUVECs were incubated with purified GAG (1 μg/mL). As a control, uninfected HUVEC monolayers were maintained under the same conditions. Briefly, after the interactions assay, the endothelial cells were washed twice with Hank's balanced salt solution (Cultilab) and gently harvested using a cell scraper. Next, the cells were centrifuged at 200 ×*g* for 10 min. The pellet was suspended in 250 μL of lysis buffer (8 M urea, 1 M Tris, 4% (*w*/*v*) CHAPS, supplemented with 1 mM PMSF, 5 mM EDTA, 160 μM leupeptin, 1 μM pepstatin, 0.125 units/μL benzonase) and incubated at 4 °C for 1 h. The cell lysate was centrifuged at 13,000 ×*g* at 4 °C for 15 min, and the supernatant (protein extract) was collected and stored at −80 °C.

2.7.2. Label-free protein analysis by mass spectrometry, database searching and quantification

Independent biological replicates (n = 3) of each experimental condition were considered for HDMS^E analysis. After extraction, the proteins were quantified using the Bradford assay and analyzed as previously described [27,28].

Protein identification and quantitative data packaging were performed using dedicated algorithms [29,30] and by searching against a database with default parameters for ion accounting and quantitation [30,31]. To assess the false positive rate of identification, the utilized databases were reversed "on the fly" during the database queries (67,911 entries) and appended to the original database. For proper spectral processing and database searching conditions, the peak list-generating software and search engine included at Progenesis QI for Proteomics software package v.2.0 (Non-Linear Dynamics, Liverpool, UK) were used. The UNIPROT protein databank release 2015_03 [32] with specific annotations for humans was used, and the search conditions were based on taxonomy (*Homo sapiens*): the maximum number of allowed missed cleavages by trypsin was set to 1; the precursor mass tolerance was set to 10 ppm and the mass tolerance for fragment ions to 20 ppm; variable modifications by carbamidomethyl (C), acetyl N-terminal, and oxidation (M) were allowed; the default FDR value was set to a maximum of 4% calculated by the Progenesis QIP software. Statistical analyses were performed with the quantitative measurements of at least 1 proteotypic peptide per protein according to the standard Progenesis QIP processing capability through ANOVA. The identified proteins were organized by the software algorithm into a statistically significant list (ANOVA p value ≤0.05) corresponding to increased and/or decreased regulation ratios. For comparing pairs of experimental groups, a cut-off Log2ratio value of +1.0 (2-fold) or higher was applied for determining those proteins with higher abundance levels, with −1.0 (2-fold) or lower for proteins with lower abundance levels [33–58]. Protein interactions and pathways were analyzed *in silico* using QIAGEN's Ingenuity® Pathway Analysis (IPA®, QIAGEN Redwood City, www.qiagen.com/ingenuity). For enrichment analysis of our dataset, we used the functional annotation tool of DAVID Bioinformatics Resources 6.7, NIAID/NIH [59]. The mass spectrometry proteomics data have been deposited in the ProteomeXchange Consortium [60] via the PRIDE [61] partner repository with the dataset identifier PXD002823.

3. Results

3.1. A. fumigatus Δugm1 strain is hyperadherent to HUVECs

A problem frequently observed in studies using cell lines is that this model does not well reflect the host-to-host variation in response to pathogens. The primary HUVEC model is used as a reference model in the vascular literature, and this aspect can be rather critical when studying infectious diseases. For example, an endothelial cell line (HMEC-1) does not respond to *Candida albicans* infection in a manner similar to the HUVEC model, showing that HUVECs can provide a more confident profile that better correlates with *in vivo* infection [62]. The present work is also based on previous results from our group that established the interaction model of endothelial cells with *A. fumigatus* hyphae [8]. For these reasons, the primary HUVEC model was used in this work to examine the endothelial response to *A. fumigatus* infection.

A differential fluorescence assay was performed to investigate the adhesion and internalization properties of *Δugm1* to human endothelial cells. After 45 min of interaction, germlings of the Δ*ugm1* strain showed an increased capacity ($p < 0.05$) to adhere to endothelial cells when compared to the capacities of the WT and *Δugm1*::*ugm1* strains. In contrast, the rate of internalization was similar for all *A. fumigatus* strains (Fig. 1).

3.2. A. fumigatus Δugm1 increases the secretion of cytokines by endothelial cells and modulates tissue factor expression

To evaluate the capacity of Δ*ugm1* to stimulate cytokine and chemokine release by endothelial cells, a kinetics assay was performed upon HUVEC: *A. fumigatus* interaction for 4, 8 and 16 h; IL-6, TNF-α and IL-8 production was quantified at each time point. The kinetics assay showed that cytokine secretion during HUVEC interaction with the *A.*

Please cite this article as: G.W.P. Neves, et al., Modifications to the composition of the hyphal outer layer of *Aspergillus fumigatus* modulates HUVEC proteins related to inflammatory and stress responses..., J Prot (2016), http://dx.doi.org/10.1016/j.jprot.2016.06.015

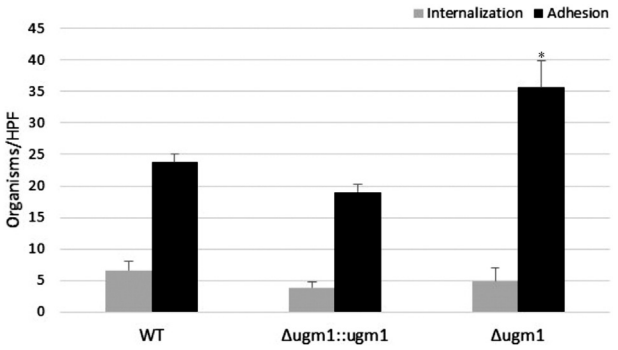

Fig. 1. *A. fumigatus* adhesion and internalization by HUVECs. Germlings of WT, mutant (*Δugm1*) and complemented (*Δugm1*::*ugm1*) strains were incubated with HUVECs for 45 min at 37 °C in 5% CO_2. The number of germlings adhered to HUVECs was determined by a differential fluorescence assay, as previously described (see Materials and methods). The results are presented as the mean ± SEM of three independent experiments performed in duplicate or triplicate. $^{*}p < 0.05$ versus WT. HPF — high-power field.

fumigatus strains was time dependent and that the highest stimulation time point was achieved at 16 h (data not shown). For this reason, a comparative analysis of cytokine release was performed after 16 h of HUVEC:*A. fumigatus* interaction. The *Δugm1* strain was able to stimulate approximately 3- and 10-fold increases in the secretion of IL-6 and TNF-α, respectively (Fig. 2). In contrast, although IL-8 secretion by HUVECs was significantly increased after infection with *A. fumigatus* germlings, no significant differences in chemokine levels induced by the wild-type, *Δugm1* and *Δugm1*::*ugm1* strains were observed (Fig. 2).

Additionally, the conidia of all three strains were not able to cause significant HUVEC cytokine release after host cell infection, in agreement with the lack of cell wall modifications to the conidial surface of the mutant [18] (data not shown). Tissue factor (CD-142) is a marker of the pro-thrombotic phenotype of endothelial cells [8]. Interestingly, real-time RT-PCR revealed that endothelial cell infection by the *Δugm1* strain led to an approximately 2.5-fold increase in tissue factor mRNA expression compared to the expression levels observed for the WT and *Δugm1*::*ugm1* strains (Fig. 2).

No significant differences in HUVEC viability were observed after 16 h of interaction with any *A. fumigatus* strain (expressed as a percentage of the uninfected control): WT, 67% ± 5%; *Δugm1*, 57% ± 8%; *Δugm1*::*ugm1*, 85% ± 5%. The levels of endothelial injury were determined according to published data using *A. fumigatus* wild-type strain Af293 [8,27], with the results indicating no relationship of cytokine induction with differences in HUVEC killing by the different strains.

3.3. Proteomic profiling of human endothelial cells challenged with A. fumigatus strains (WT and Δugm1)

Because our results indicated a significant change in the endothelial response to the *Δugm1* strain, a shotgun proteomics approach was performed to compare differences at the protein level of HUVECs challenged with the *Δugm1* and WT strains of this angioinvasive fungus. For this analysis, three pairs of comparisons were performed between experimental groups: (i) HUVECs challenged with the WT strain vs. uninfected HUVECs (WT vs. control); (ii) HUVECs challenged with the *Δugm1* strain vs. uninfected HUVECs (*Δugm1* vs. control); and (iii) HUVECs challenged with the *Δugm1* strain vs. HUVECs challenged with the WT strain (*Δugm1* vs. WT). We identified 750, 650 and 706 proteins for comparisons i, ii and iii, respectively, using the cut-off values of 2-fold (Log(2)ratio ≥ +1.0, for proteins with higher abundance levels and ≤−1.0 for proteins with lower abundance levels) and the ANOVA *p*-value. The proteomic profile using uninfected HUVECs as a reference showed that compared to the WT strain, *Δugm1* was responsible for an alteration in the abundance of 30% more proteins (Fig. 3).

Applying the 2-fold abundance ratio and a quantification ANOVA *p*-value ≤0.05, 18 and 26 proteins presented differences in the abundance

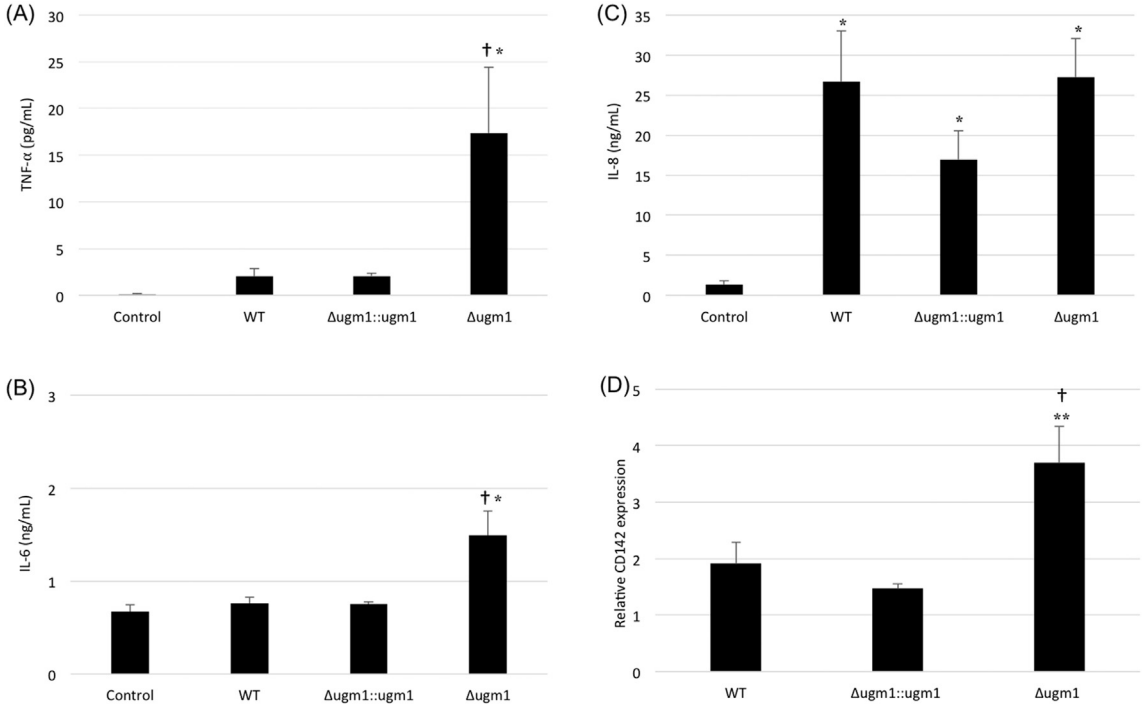

Fig. 2. HUVEC activation profile after 16 h of interaction with *A. fumigatus* germlings. HUVECs were infected with the WT, *Δugm1* and *Δugm1*::*ugm1* strains. The HUVEC conditioned medium was collected and assayed for TNF-α (A), IL-6 (B) and IL-8 (C). Expression of the CD142 gene was normalized to GAPDH, and the results are expressed as the increase in expression relative to the expression level measured for uninfected endothelial cells (D). The results are presented as the mean ± SEM of at least two independent experiments performed in duplicate or triplicate. $^{*}p < 0.05$ versus uninfected control; $^{**}p < 0.001$ compared with the uninfected control, † $p < 0.05$ versus endothelial cells infected with the WT and complemented strains.

Please cite this article as: G.W.P. Neves, et al., Modifications to the composition of the hyphal outer layer of *Aspergillus fumigatus* modulates HUVEC proteins related to inflammatory and stress responses..., J Prot (2016), http://dx.doi.org/10.1016/j.jprot.2016.06.015

ratio of HUVECs challenged with *A. fumigatus*. The abundance of 18 proteins was altered in HUVECs challenged with the WT strain, with 12 proteins showing lower abundance levels and 6 higher abundance levels (Fig. 3B). When these endothelial cells were challenged with the Δ*ugm1* mutant, 26 proteins were found to have altered abundance, with 19 showing lower abundance levels and 7 higher abundance levels (Fig. 3B). All proteins found to be altered in abundance under both conditions are listed in Table 1. As shown by the Venn's diagram, 6 proteins were commonly modulated in HUVECs infected with both *A. fumigatus* strains (Fig. 3B). These common proteins were high mobility group protein B1, enhancer of rudimentary homolog, calponin-3, glial fibrillary acidic protein, ras-related protein Rab-3D and T-complex protein 1 subunit epsilon.

In this work, we used only biological replicates of HUVEC primary cultures from different human donors (of various ages, ethnicities, genomic backgrounds and other factors) rather than using technical replicates of proteins pools [63]; thus, we decided to complement the data using a less stringent analysis [28] to avoid the loss of important biological information. For this supplementary analysis, we only considered a 2-fold abundance ratio without the ANOVA *p*-value, and surprisingly, the same percentages of modulated proteins were observed (Fig. 3A). All these proteins with putative different abundance levels are listed in Table 1 in reference [28]. Furthermore, the qualitative information regarding these proteins highlighted the *ILK* and *mTOR signaling* pathways (see Fig. 4 in Ref. [28]). Interestingly, the proteins involved in these pathways were statistically validated (ANOVA *p*-value ≤ 0.05) when the HUVECs interacted with the *A. fumigatus* cell wall-purified polysaccharide, which is overexpressed in the Δ*ugm1* mutant, as discussed below.

3.4. *A. fumigatus* Δugm1 regulates important and specific HUVEC pathways

Compared to the *A. fumigatus* WT strain, the *UGM1* mutant overexpresses the GAG component of the cell wall. For this reason, we compared modulated proteins in HUVEC monolayers infected with both strains. Table 1 shows the list of statistically significant proteins with abundance differences identified in the interaction conditions of Δ*ugm1* vs. control, WT vs. control and Δ*ugm1* vs. WT. Taking into account the direct comparison of relative HUVEC protein abundance levels between Δ*ugm1* and WT after 16 h of interaction (Δ*ugm1* vs. WT), 12 proteins were statistically validated (ANOVA *p*-value ≤ 0.05) and modulated by Δ*ugm1* (Table 1). Among them, 3 HUVEC proteins were commonly modulated by both strains.

When considering the statistically validated HUVEC proteins modulated by the Δ*ugm1* mutant (Δ*ugm1* vs. WT), regulation of the following is highlighted: (i) blood coagulation and immune response - 1-phosphatidylinositol 4.5-bisphosphate phosphodiesterase gamma-2 [64,65]; (ii) immune response - 26S protease regulatory subunit 6B [66]; (iii) stress response and unfolded protein response - heat-shock-related 70 kDa protein 2 [67] and (iv) apoptotic process and response to stress - reticulon-3 [68] (see all proteins in Table 1).

Moreover, to unveil the specific pathways regulated by the Δ*ugm1* mutant, Ingenuity Pathway Analysis (IPA) was performed with the list of HUVEC proteins modulated under the conditions Δ*ugm1* vs. control and Δ*ugm1* vs. WT (Table 1). This analysis revealed that some endothelial pathways were regulated by Δ*ugm1* either compared to the HUVEC control or to the HUVEC infected with the WT strain condition (Δ*ugm1* vs. control and Δ*ugm1* vs. WT), as shown in Fig. 4 and Table 2. Only proteins with higher abundance levels in both experimental comparisons were observed for *unfolded protein response* and *eNOS signaling* pathways. Nonetheless, proteins involved in the *14-3-3 signaling* and *protein ubiquitination* pathways showed both higher and lower abundance levels, which may reflect a more refined control.

Fig. 5 illustrates that the 14-3-3 mediated signaling pathway is differentially regulated under the Δ*ugm1* interaction condition; this image was generated by IPA and shows that this pathway can be regulated by TNF-α, leading to activation of ELK-1 (ETS domain-containing

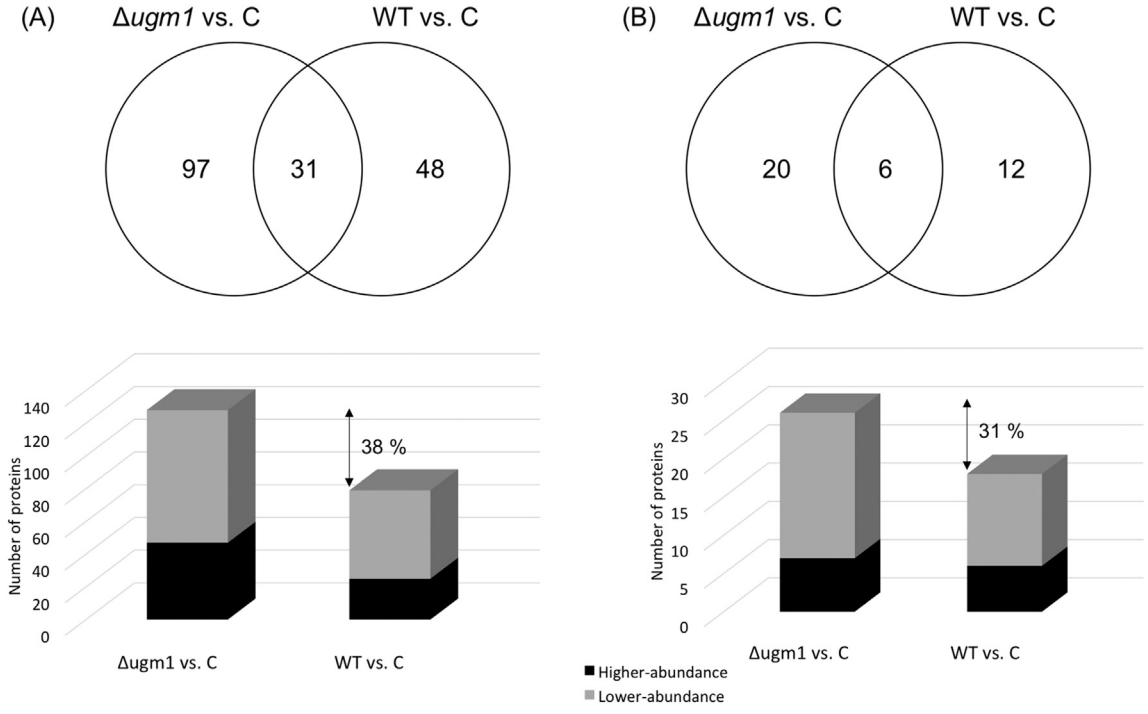

Fig. 3. Quantitative comparative analysis of proteins showing different abundance levels in HUVECs after interaction with the mutant (Δ*ugm1* vs. control) and the wild-type strain (WT vs. control) of *A. fumigatus*, before and after applying the quantitation ANOVA *p*-value ≤ 0.05 as a cut-off. (B) The Venn diagram shows the number of proteins commonly found in both Δ*ugm1* vs. control and WT vs. control comparisons (intersection) or modulated only in one of the comparisons. The graph illustrates the number of proteins with higher or lower abundance levels in both comparisons. In this quantitative analysis, we used as a cut-off only statistically validated proteins, with quantitation criteria of a minimum of a 2.0 fold-change and an ANOVA *p*-value ≤ 0.05. (A) The Venn diagram shows the number of proteins found in both Δ*ugm1* vs. control and WT vs. control comparisons (intersection) or modulated only in one of the comparisons. The graph illustrates the number of proteins with higher or lower abundance levels in the Δ*ugm1* vs. control and WT vs. control comparisons. For this quantitative analysis, we used only the 2.0 fold-change criterion.

Please cite this article as: G.W.P. Neves, et al., Modifications to the composition of the hyphal outer layer of *Aspergillus fumigatus* modulates HUVEC proteins related to inflammatory and stress responses..., J Prot (2016), http://dx.doi.org/10.1016/j.jprot.2016.06.015

Table 1
List of proteins differentially regulated in the WT vs. control (WT:C) comparison, Δugm1 vs. control (Δ:C) comparison and Δugm1 vs. WT (Δ:WT) comparison.

WT vs. C				
Accession number[a]	Protein identification[a]	Biological process [a]	WT:C Log(2) ratio[b]	ANOVA p-value
P09493	Tropomyosin alpha-1 chain	cellular response to reactive oxygen species; positive regulation of cell adhesion; wound healing	-1.9	0.03
Q8TF09	Dynein light chain roadblock-type 2	transport	-1.7	0.03
Q9UI15	Transgelin-3	negative regulation of transcription from RNA polymerase II promoter	-1.6	0.03
P30461	HLA class I histocompatibility antigen. B-13 alpha chain	antigen processing and presentation of exogenous peptide antigen via MHC class I; interferon-gamma-mediated signaling pathway; regulation of immune response	-1.5	0.01
Q9BWF3	RNA-binding protein 4	cell differentiation; stress-activated MAPK cascade	-1.5	0.04
Q9UBV8	Peflin	proteolysis	-1.2	0.00
P09429	High mobility group protein B1	activation of innate immune response; adaptive immune response; apoptotic process; inflammatory response to antigenic stimulus; positive regulation of interferon-alpha production; positive regulation of interferon-beta production; positive regulation of interleukin-1 beta secretion; positive regulation of interleukin-6 secretion; positive regulation of JNK cascade; positive regulation of monocyte chemotaxis; positive regulation of sprouting angiogenesis; positive regulation of tumor necrosis factor production; positive regulation of wound healing	-1.2	0.00
Q16270	Insulin-like growth factor-binding protein 7	cell adhesion; negative regulation of cell proliferation	-1.2	0.00
Q15417	Calponin-3	epithelial cell differentiation	-1.1	0.02
Q9BWJ5	Splicing factor 3B subunit 5	RNA splicing	-1.1	0.02
P84090	Enhancer of rudimentary homolog	cell cycle; positive regulation of Notch signaling pathway	-1.1	0.01
Q9UBR2	Cathepsin Z	angiotensin maturation; proteolysis	-1.0	0.00
P02656	Apolipoprotein C-III	regulation of Cdc42 protein signal transduction	1.3	0.00
Q12799	T-complex protein 10A homolog	not defined	2.0	0.03
P13646	Keratin. type I cytoskeletal 13	cytoskeleton organization	2.1	0.02
P48643	T-complex protein 1 subunit epsilon	protein folding; toxin transport	2.7	0.00
P14136	Glial fibrillary acidic protein	extracellular matrix organization; response to wounding	3.7	0.01
O95716	Ras-related protein Rab-3D	exocytosis; positive regulation of regulated secretory pathway	4.6	0.01
Δugm1 vs. C				
Accession number[a]	Protein identification[a]	Biological process [a]	Δ:C Log(2) ratio[b]	ANOVA p-value
P19105; O14950; P24844	Myosin regulatory light chain 12A; Myosin regulatory light chain 12B; Myosin regulatory light polypeptide 9	small GTPase mediated signal transduction; regulation of cell shape; platelet aggregation	-1.1	0.03
P61088; Q5JXB2	Ubiquitin-conjugating enzyme E2 N; Putative ubiquitin-conjugating enzyme E2 N-like	cytokine-mediated signaling pathway; innate immune response; MyD88-dependent toll-like receptor signaling pathway; positive regulation of I-kappaB kinase/NF-kappaB signaling; positive regulation of NF-kappaB transcription factor activity; proteolysis; stimulatory C-type lectin receptor signaling pathway; T cell receptor signaling pathway	-1.1	0.02
Q15417	Calponin-3	epithelial cell differentiation	-1.1	0.02
Q92804	TATA-binding protein-associated factor 2N	positive regulation of transcription	-1.1	0.03
P31150	Rab GDP dissociation inhibitor alpha	negative regulation of protein targeting to membrane; protein transport; signal transduction	1.3	0.03
Q01664	Transcription factor AP-4	negative regulation of cell proliferation; positive regulation of apoptotic process	1.4	0.04
P54652	Heat shock-related 70 kDa protein 2	response to unfolded protein	1.4	0.01
P14136	Glial fibrillary acidic protein	extracellular matrix organization; response to wounding	1.7	0.03

Please cite this article as: G.W.P. Neves, et al., Modifications to the composition of the hyphal outer layer of *Aspergillus fumigatus* modulates HUVEC proteins related to inflammatory and stress responses..., J Prot (2016), http://dx.doi.org/10.1016/j.jprot.2016.06.015

P35241	Radixin	establishment of endothelial barrier; establishment of protein localization to plasma membrane; regulation of cell shape; regulation of cell size	2.4	0.04
O95716	Ras-related protein Rab-3D	exocytosis; positive regulation of regulated secretory pathway	2.7	0.05
P48643	T-complex protein 1 subunit epsilon	protein folding; toxin transport	4.5	0.03
P30049	ATP synthase subunit delta. mitochondrial	respiratory electron transport chain; small molecule metabolic process	-2.1	0.02
P17900	Ganglioside GM2 activator	small molecule metabolic process	-2.1	0.01
Q14257	Reticulocalbin-2	not defined	-1.8	0.03
Q13561	Dynactin subunit 2	antigen processing and presentation of exogenous peptide antigen via MHC class II; mitotic cell cycle; organelle organization	-1.8	0.02
P09429	High mobility group protein B1	activation of innate immune response; adaptive immune response; apoptotic process; inflammatory response to antigenic stimulus; positive regulation of interferon-alpha production; positive regulation of interferon-beta production; positive regulation of interleukin-1 beta secretion; positive regulation of interleukin-6 secretion; positive regulation of JNK cascade; positive regulation of monocyte chemotaxis; positive regulation of sprouting angiogenesis; positive regulation of tumor necrosis factor production; positive regulation of wound healing	-1.6	0.04
P10606	Cytochrome c oxidase subunit 5B. mitochondrial	respiratory electron transport chain; small molecule metabolic process	-1.6	0.03
O75380	NADH dehydrogenase [ubiquinone] iron-sulfur protein 6. mitochondrial	mitochondrion morphogenesis; respiratory electron transport chain; small molecule metabolic process	-1.4	0.03
P39687	Acidic leucine-rich nuclear phosphoprotein 32 family member A	gene expression; intracellular signal transduction	-1.4	0.00
P37802	Transgelin-2	epithelial cell differentiation	-1.4	0.02
O75947	ATP synthase subunit d. mitochondrial	respiratory electron transport chain; small molecule metabolic process	-1.3	0.04
P28799	Granulins	positive regulation of epithelial cell proliferation; signal transduction	-1.3	0.02
Q9H299	SH3 domain-binding glutamic acid-rich-like protein 3	cell redox homeostasis; regulation of actin cytoskeleton organization; regulation of blood vessel endothelial cell migration	-1.3	0.01
Q9HAV7	GrpE protein homolog 1. mitochondrial	protein folding; protein targeting to mitochondrion	-1.3	0.01
P84090	Enhancer of rudimentary homolog	cell cycle; positive regulation of Notch signaling pathway	-1.1	0.03
Q9Y5J7	Mitochondrial import inner membrane translocase subunit Tim9	protein import into mitochondrial inner membrane	-1.1	0.04
		Δugm1 vs. WT		
Accession number[a]	**Protein identification**[a]	**Biological process**[a]	**Δ:WT Log(2) ratio**[b]	**ANOVA p-value**
O95716	Ras-related protein Rab-3D	exocytosis; positive regulation of regulated secretory pathway	-2.0	0.04
P43686	26S protease regulatory subunit 6B	antigen processing and presentation of exogenous peptide antigen via MHC class I; innate immune response; NIK/NF-kappaB signaling; regulation of apoptotic process; T cell receptor signaling pathway	-1.9	0.02
Q9UK76	Hematological and neurological expressed 1 protein	not defined	-1.8	0.01
P02656	Apolipoprotein C-III	regulation of Cdc42 protein signal transduction	-1.6	0.00
Q14847	LIM and SH3 domain protein 1	positive regulation of signal transduction	-1.6	0.02
O60664	Perilipin-3	vesicle-mediated transport	-1.1	0.02
P12035	Keratin. type II cytoskeletal 3	epithelial cell differentiation; intermediate filament cytoskeleton organization	-1.0	0.01
O95197	Reticulon-3	apoptotic process; response to stress; vesicle-mediated transport	1.0	0.02
P54652	Heat shock-related 70 kDa protein 2	response to unfolded protein	1.3	0.02
P16885	1-phosphatidylinositol 4.5-bisphosphate phosphodiesterase gamma-2	B cell differentiation; B cell receptor signaling pathway; blood coagulation; innate immune response; platelet activation; T cell receptor signaling pathway	1.7	0.01
Q9Y2Q3	Glutathione S-transferase kappa 1	epithelial cell differentiation; oxidation-reduction process	1.8	0.05

[a] Data obtained from UniProt Knowledgebase (UniProtKB)

[b] Log(2)ratio values considered statistically significant ($p \leq 0.05$). The cut off values were at least equal or bigger than +1.0, for higher-abundance level proteins, and equal or smaller than -1.0, for lower-abundance level proteins.

protein Elk-1) and p73 (tumor protein p73), two transcription factors related to the inflammatory response. Finally, these results correlated well with the increase in TNF-α secretion by HUVECs in response to Δ*ugm1* and to purified GAG.

For the same reason as discussed above, i.e., the use of biological replicates instead of technical replicates [63], we also performed a less stringent IPA analysis using proteins filtered only with the 2-fold change criterion. This analysis suggested that the Δ*ugm1* mutant may also

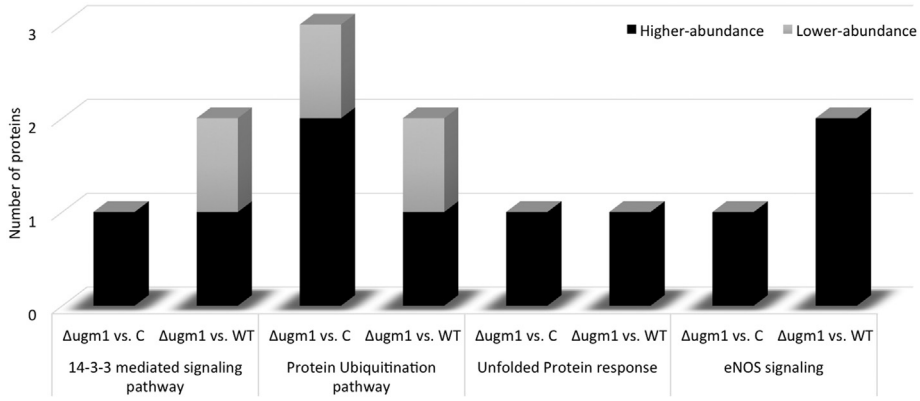

Fig. 4. Ingenuity pathway analysis showing commonly regulated pathways in the Δ*ugm1* vs. control and Δ*ugm1* vs. WT comparisons. The graph shows the main pathways regulated by Δ*ugm1*, indicating the number of proteins classified as up and down according to their abundance levels under the Δ*ugm1* interaction condition (higher or lower abundance levels, respectively). For this analysis, we used only proteins validated according to the following quantitation criteria: minimum of 2.0 fold-change and ANOVA *p*-value ≤ 0.05.

cause modulation of the abundance of HUVEC proteins involved in immune, inflammatory and stress responses, with the following pathways being regulated: *14-3-3 mediated signaling*, *epithelial adherence junction signaling*, *actin cytoskeleton signaling*, *remodeling epithelial adherence junction signaling*, *regulation of actin-based motility by Rho*, *agranulocyte adhesion and diapedesis*, *CDC42 signaling*, *protein ubiquitination pathway*, *antigen presentation pathway* (See Fig. 3 in Ref. [28]). All these proteins (2-fold change criteria) are listed in Tables 1 and 2 in reference [28].

Moreover, it is important to highlight that *A. fumigatus* Δ*ugm1* not only overexpresses GAG but also lacks the galactomannan found in the cell wall of the WT strain [18]. Accordingly, we tested purified GAG isolated from *A. fumigatus* (see Materials and methods).

Table 2
List of HUVEC differentially regulated proteins found in pathways commonly predicted by the IPA in both experimental conditions Δ*ugm1* vs. control (Δ:C) and/or Δ*ugm1* vs. WT (Δ:WT).

Accession number[a]	Protein name[a]	Δ:C_Log(2) ratio[b]	Δ:WT_Log(2) ratio[b]
14-3-3 mediated signaling			
P14136	Glial fibrillary acidic protein	1.7	−1.9
P16885	1-phosphatidylinositol 4,5-bisphosphate phosphodiesterase gamma-2	[e]	1.7
Unfolded protein response			
P54652	Heat shock-related 70 kDa protein 2	1.4	1.3
Protein ubiquitination pathway			
P54652	Heat shock-related 70 kDa protein 2	1.4	1.3
P43686	26S protease regulatory subunit 6B	1.7	−1.9
P61088	Ubiquitin-conjugating enzyme E2 N	−1.1	[d]
eNOS signaling			
P54652	Heat shock-related 70 kDa protein 2	1.4	1.3
P16885	1-phosphatidylinositol 4,5-bisphosphate phosphodiesterase gamma-2	[e]	1.7

[a] Data obtained from UniProt Knowledgebase (UniProtKB).
[b] Log(2)ratio values considered statistically significant ($p \leq 0.05$). The cut off values were at least equal or bigger than +1.0, for higher-abundance level proteins, and equal or smaller than −1.0, for lower-abundance level proteins.
[d] Protein not filtered by the minimum of 2.0 fold-change criteria.
[e] Protein not identified in one of the experimental conditions.

3.5. The A. fumigatus cell surface component GAG induces TNF-α secretion by HUVECs and regulates endothelial pathways found in the Δugm1 interaction condition

In contrast to the parental (WT) and complemented *Δugm1*::*ugm1* strains, *A. fumigatus* Δ*ugm1* germlings and swollen conidia exhibit more abundant surface material (see Fig. 1A in Ref. [28]). In agreement with Gravelat et al. [20], fluorescence microscopy using anti-GAG antibodies and TRITC-conjugated secondary antibodies confirmed that this abundant extracellular material corresponds to a higher GAG content; lower fluorescence is found in the WT strain (see Fig. 1B in Ref. [28]). This result indicates that *Δugm1* produces more GAG than the parental strain, suggesting that the extracellular material involved in *A. fumigatus* adherence to endothelial cells is GAG, as shown in Fig. 1.

We thus addressed whether the response of HUVEC cells to the Δ*ugm1* mutant is more likely caused by the presence of GAG than the lack of GM as a consequence of the *UGM1* deletion. To investigate the role of GAG in the HUVEC response, endothelial cells were incubated directly with GAG. The level of cytokines in the HUVEC-conditioned medium after 16 h of interaction with GAG indicated that this polysaccharide was able to induce a statistically significant increase in TNF-α secretion. When HUVECs interacted with GAG, the levels of TNF-α secretion were 12.72 pg/mL ± 4.57 compared to 2.01 pg/mL ± 0.87 for the WT interaction condition; 0.07 pg/mL ± 0.16 was observed for the HUVEC control. In this case, cellulose was used as a control because previous studies have shown that only water-insoluble cell wall polysaccharides are able to induce an immune response (Latgé JP et al., unpublished data), with no induction of cytokine secretion (undetected level) by HUVECs.

Regarding the shotgun proteomics analysis of HUVECs challenged with GAG, 763 proteins were identified in the GAG vs. control comparison. Among these, 26 proteins showed different abundance levels (2-fold change and ANOVA *p*-value ≤ 0.05), as shown in Table 3. Interestingly, the abundance of the majority of these proteins was lower under the GAG interaction condition. To unveil pathways that might be specifically regulated by GAG, IPA analysis was performed to identify the common pathways regulated by both GAG and Δ*ugm1* in HUVECs. This analysis revealed five pathways commonly found in the HUVEC response under both experimental conditions, with all proteins presenting lower abundance levels (Table 4 and Fig. 6). Of note, these pathways are involved in oxidative stress and infectious disease responses: *oxidative phosphorylation*, *mitochondrial dysfunction*, *chondroitin sulfate degradation*, *dermatan sulfate degradation and hypoxia signaling in the cardiovascular system*.

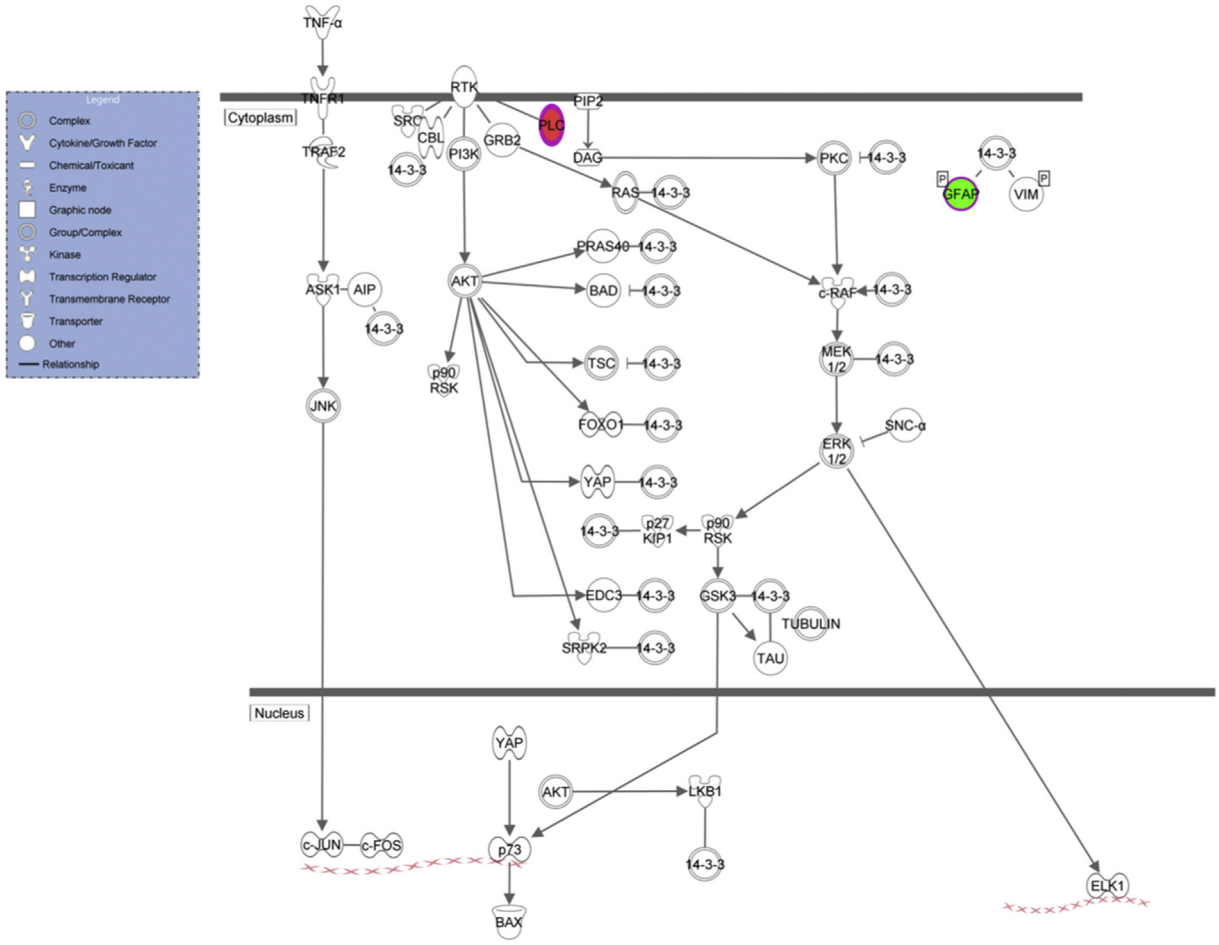

Fig. 5. Illustration of the 14-3-3-mediated signaling pathway generated by QIAGEN's Ingenuity® Pathway Analysis and regulated by Δ*ugm1*. Proteins in red and green indicate higher and lower abundance levels under the mutant interaction condition, respectively. In addition, the figure illustrates that TNF-α can participate in the upstream regulation of this pathway. The arrows indicate the predicted regulation: activation (→) or inhibition (⊢). The proteins used in this analysis were filtered according to the following quantitation criteria: minimum of 2.0 fold-change and ANOVA *p*-value ≤ 0.05. TNF — Tumor Necrosis Factor; TNFR1 — Tumor Necrosis Factor Receptor Superfamily Member 1 A; TRAF2 — Tumor Necrosis Factor Receptor Associated Factor 2; ASK1 — Mitogen-Activated Protein Kinase 5; JNK — c-Jun N-terminal Protein Kinase; cJUN — Jun Proto-Oncogene; cFOS — FBJ Murine Osteosarcoma viral oncogene homolog; YAP — Yes-Associated Protein 1; P73 — Tumor Protein P73; BAX — BCL2-associated X Protein; AKT — Protein Kinase B; LKB1 — Serine/Threonine Kinase 11; 14-3-3–14-3-3 Protein; EDC3 — Enhancer of mRNA decapping 3; SRPK2 — SRSF Protein Kinase 2; AiP — Programed Cell Death 6-Interacting Protein; p90RSK — Ribosomal Protein S6 Kinase 90 kDa Polypeptide 1; TSC — Tuberous Sclerosis Complex Protein; FOX01 — Fork head box 01; BAD — BLC2-Associated Agonist of Cell Death; P13K — 1 Phosphatidylinositol 3 kinase; SRC — SRC Proto-oncogene; RTK — Receptor Tyrosine Kinase; GRB2 — Growth Factor Receptor-binding Protein 2; PIP2 — 1-Phosphatidyl-1D-myo-inositol 4,5 bisphosphate; PLC — Phospholipase C; DAG — Diacylglycerol; PRAS40 — AKT1 substrate 1; PKC — Protein Kinase C; Ras — Ras Protein; CRAF — Raf 1 Proto-oncogene Serine/Threonine Kinase; MEK1/2 — Mitogen-activated Protein Kinases MEK1/2; GFAP — Glial Fibrillary Acid Protein; VIM — Vimentin; SNCα — Synuclein α; ERK ½ — Mitogen-activated Protein Kinases ERK 1/2; TUBULIN — Tubulin Complex; P27KIP1 — Cyclin-dependent Kinase inhibitor 1B; GSK3 — Glycogen synthase kinase 3; TAU — Microtubule-associated Protein TAU; LKB1 — Serine/Threonine Kinase 11; LBL — Lbl Proto-oncogene/E3 ubiquitin Protein ligase.

These results were corroborated by the enrichment analysis of our dataset performed by DAVID Bioinformatics Resources 6.7 [59], which validated the observed regulation of *Oxidative phosphorylation pathway* (*p*-value = 0.0017) under the Δ*ugm1* interaction condition. This pathway was also revealed in the DAVID analysis performed for the GAG interaction condition. According to this analysis, the proteins involved in *Oxidative phosphorylation pathway* are ATP synthase subunit delta, cytochrome *c* oxidase subunit 5B, ATP synthase subunit d, NADH dehydrogenase [ubiquinone] iron-sulfur protein 6, the same proteins according to IPA for this pathway, as shown in Table 4. This pathway is illustrated in Fig. 7. Furthermore, DAVID analysis validated *lysosome pathway* (*p*-value = 0.021) for the GAG interaction condition, involving GM2 ganglioside activator, beta-hexosaminidase subunit beta and cathepsin Z. Interestingly, 2 of these proteins are involved in the *chondroitin sulfate degradation* and *dermatan sulfate degradation* pathways according to IPA (Table 4). *Lysosome pathway* was also indicated by the DAVID analysis for the Δ*ugm1* interaction condition, but only involving the GM2 ganglioside activator.

Moreover, the GO enrichment analysis for biological processes by DAVID indicated the following statistically validated terms (*p*-value ≤ 0.05): mitochondrial transport, oxidative phosphorylation and protein localization for the Δ*ugm1* interaction condition; and oligosaccharide metabolic process, ganglioside metabolic process, glycolipid metabolic process, glycosphingolipid metabolic process, membrane lipid catabolic process and lipid storage for the GAG interaction condition.

In addition, the IPA analysis of altered HUVEC proteins in response to GAG showed pathways involved in inflammatory responses, such as *mTOR signaling* and *ILK signaling* (data not shown), a result in accordance with the cytokine analysis that showed higher TNF-α secretion due to GAG. Fig. 5 in reference [28] illustrates the ILK signaling pathway generated by the IPA analysis.

To gain a better biological overview of the pathways involved in the HUVEC response to GAG, we also performed IPA analysis considering proteins filtered only by the 2-fold change criterion (see Table 3 in Ref. [28]). Interestingly, some other pathways were coincident with the Δ*ugm1* analysis: *14-3-3 mediated signaling*, *epithelial adherens*

Table 3
List of proteins differentially regulated in the GAG vs. control (GAG:C) comparison.

Accession number[a]	Protein identification[a]	Biological process[a]	GAG:C Log(2) ratio[b]	ANOVA p-value
Q9UI15	Transgelin-3	Negative regulation of transcription from RNA polymerase II promoter	−2.1	0.01
P17900	Ganglioside GM2 activator	Small molecule metabolic process	−1.7	0.02
Q15404	Ras suppressor protein 1	Positive regulation of cell-substrate adhesion; cell junction assembly; Ras protein signal transduction	−1.6	0.04
P17302	Gap junction alpha-1 protein	Apoptotic process; cell-cell signaling; chronic inflammatory response; cellular response to mechanical stimulus; endothelium development; positive regulation of I-kappaB kinase/NF-kappaB signaling; response to fluid shear stress; response to peptide hormone	−1.6	0.04
P62841	40S ribosomal protein S15	Translation; cellular protein metabolic process	−1.6	0.04
O43504	Regulator complex protein LAMTOR5	Cell cycle arrest; positive regulation of GTPase activity; positive regulation of mTOR signaling; negative regulation of apoptotic process	−1.5	0.04
P61088; Q5JXB2	Ubiquitin-conjugating enzyme E2 N; Putative ubiquitin-conjugating enzyme E2 N-like	Cytokine-mediated signaling pathway; innate immune response; MyD88-dependent toll-like receptor signaling pathway; positive regulation of I-kappaB kinase/NF-kappaB signaling; positive regulation of NF-kappaB transcription factor activity; proteolysis; stimulatory C-type lectin receptor signaling pathway; T cell receptor signaling pathway	−1.5	0.01
Q99623	Prohibitin-2	Negative regulation of apoptotic process; protein stabilization	−1.4	0.01
Q4VXU2	Polyadenylate-binding protein 1-like	mRNA polyadenylation	−1.4	0.01
Q99877; Q96A08	Histone H2B type 1-N; Histone H2B type 1-A	Chromatin organization; inflammatory response; plasminogen activation; innate immune response in mucosa	−1.4	0.05
P10606	Cytochrome *c* oxidase subunit 5B. mitochondrial	Respiratory electron transport chain; small molecule metabolic process	−1.3	0.02
P21291	Cysteine and glycine-rich protein 1	Platelet aggregation	−1.3	0.01
Q07021	Complement component 1 Q subcomponent-binding protein. Mitochondrial	Apoptotic process; blood coagulation; complement activation. Classical pathway; innate immune response; positive regulation of cell adhesion; positive regulation of dendritic cell chemotaxis; positive regulation of neutrophil chemotaxis	−1.3	0.02
P55145	Mesencephalic astrocyte-derived neurotrophic factor	Response to unfolded protein	−1.2	0.04
Q14257	Reticulocalbin-2	Not defined	−1.1	0.04
O14979	Heterogeneous nuclear ribonucleoprotein D-like	Regulation of gene expression	−1.1	0.01
P14314	Glucosidase 2 subunit beta	Innate immune response; post-translational protein modification; protein folding	−1.1	0.01
Q8WUP2	Filamin-binding LIM protein 1	Regulation of cell shape; regulation of integrin activation; single organismal cell-cell adhesion	−1.1	0.01
O43390	Heterogeneous nuclear ribonucleoprotein R	Gene expression	−1.0	0.03
P67809	Nuclease-sensitive element-binding protein 1	Gene expression; positive regulation of cell division	−1.0	0.03
P07686	Beta-hexosaminidase subunit beta	Regulation of cell shape; phospholipid biosynthetic process; chondroitin sulfate metabolic process; keratan sulfate metabolic process	−1.0	0.01
O75947	ATP synthase subunit d. mitochondrial	Respiratory electron transport chain; small molecule metabolic process	−1.0	0.04
P62851	40S ribosomal protein S25	Cellular protein metabolic process; gene expression; translation	−1.0	0.04
Q9UBR2	Cathepsin Z	Angiotensin maturation; post-translational protein modification; proteolysis	−1.0	0.00
P12882	Myosin-1	Not defined	1.8	0.01
Q99832	T-complex protein 1 subunit eta	De novo' posttranslational protein folding; cellular protein metabolic process; protein folding; toxin transport	2.5	0.04

[a] Data obtained from UniProt Knowledgebase (UniProtKB).
[b] Log(2)ratio values considered statistically significant ($p \leq 0.05$). The cut off values were at least equal or bigger than +1.0, for higher-abundance level proteins, and equal or smaller than −1.0, for lower-abundance level proteins.

signaling, *remodeling epithelial adherens signaling*, *ILK signaling*, *mTOR signaling*, *EIF2 signaling*, and *phagosome maturation* (see Fig. 4 in Ref. [28]). This analysis is in agreement with the fact that both GAG and Δ*ugm1* induce higher TNF-α secretion by HUVECs compared to the control and WT strain.

4. Discussion

During invasive aspergillosis, interaction between *A. fumigatus* and the vascular endothelium is key to understanding the physiopathology of this disease. Blood vessel invasion, thrombo-mycotic occlusion and hemorrhagic infarctions are characteristic pathological findings in patients with this high-mortality fungal disease [69]. It is well described that endothelial cells switch to a prothrombotic phenotype after interacting with *A. fumigatus* hyphae, and it is known that this is due to TNF-α secretion and tissue factor expression [7,8,9]. This endothelial phenotype is characteristic of many thrombotic and inflammatory diseases, such as septic shock [70]. However, some of the molecular mechanisms involved in the host-fungus interplay of non-phagocytic host cells have yet to be elucidated [71,72].

The cell wall of *A. fumigatus* is the first structure to come in contact with host cells. It is a complex and dynamic structure, mainly composed of polysaccharides, and that can change depending on the fungal cell morphotype [72]. Recently, a new cell wall polysaccharide, GAG, described as composing the so-called *A. fumigatus* extracellular matrix, was found to be related to the hyphal cell wall but not to the conidial cell surface [10,73,74]. It is important to note that only *A. fumigatus* hyphae are able to deeply invade host tissues by overcoming some physiological barriers [72]. Due to the location of GAG on the outer layer of *A. fumigatus* hyphae, the central hypothesis is that the molecule may play a pivotal role in the interaction of this pathogen with host cells [11]. The main goal of the present work was to evaluate the involvement of GAG in the endothelial interaction and response to *A. fumigatus* infection.

The experimental strategy was to compare the HUVEC proteome in response to *A. fumigatus* strain Δ*ugm1* and WT. Furthermore, the HUVEC proteome in response to a purified GAG fraction was also

Table 4
List of HUVEC differentially regulated proteins found in pathways commonly predicted by the IPA in both experimental conditions Δ*ugm1* vs. control (Δ:C) and/or GAG vs. C (GAG:C).

Accession number[a]	Protein name[a]	Δ:C Log(2) ratio[b]	GAG:C Log(2) ratio[b]
Oxidative phosphorylation			
P30049	ATP synthase subunit delta, mitochondrial	−2.133	[c]
O75947	ATP synthase subunit d, mitochondrial	−1.313	−0.971
P10606	Cytochrome *c* oxidase subunit 5B, mitochondrial	−1.581	−1.322
O75380	NADH dehydrogenase [ubiquinone] iron-sulfur protein 6, mitochondrial	−1.408	[d]
Mitochodrial dysfunction			
P30049	ATP synthase subunit delta, mitochondrial	−2.133	[c]
O75947	ATP synthase subunit d, mitochondrial	−1.313	−0.971
P10606	Cytochrome *c* oxidase subunit 5B, mitochondrial	−1.581	−1.322
O75380	NADH dehydrogenase [ubiquinone] iron-sulfur protein 6, mitochondrial	−1.408	[d]
Chondroitin Sulfate Degradation			
P17900	Ganglioside GM2 activator	−2.082	−1.72
P07686	Beta-hexosaminidase subunit beta	[d]	−1.013
Dermatan sulfate degradation			
P17900	Ganglioside GM2 activator	−2.082	−1.72
P07686	Beta-hexosaminidase subunit beta	[d]	−1.013
Hypoxia signaling in the cardiovascular system			
P61088	Ubiquitin-conjugating enzyme E2 N	−1.118	−1.453

[a] Data obtained from UniProt Knowledgebase (UniProtKB).
[b] Log(2)ratio values considered statistically significant ($p \leq 0.05$). The cut off values were at least equal or bigger than +1.0, for higher-abundance level proteins, and equal or smaller than −1.0, for lower-abundance level proteins.
[c] Protein not filtered by the minimum of 2.0 fold-change criteria.
[d] Protein not identified in one of the experimental conditions.

analyzed. The Δ*ugm1* strain lacks Gal*f* residues [18] and shows an increased cell surface content of GAG (See Fig. 1 in Ref. [28]). In agreement with our hypothesis, the results showed a hyperadhesive phenotype of Δ*ugm1* germlings to HUVECs, correlating with increased endothelial secretion of IL-6 and TNF-α and a pro-thrombotic phenotype characterized by a 2.5-fold increase in tissue factor expression. Interestingly, these results correlated with the ability of the purified polysaccharide to induce an almost 6-fold increase in TNF-α secretion by HUVECs. Our findings are in line with previous reports indicating that GAG is a major adhesin of *A. fumigatus* and an immunomodulatory molecule [20,21,22,75,76].

In addition, the purified GAG and Δ*ugm1* strain both modulated the abundance of key HUVEC proteins involved in inflammatory and stress responses. IPA indicated five pathways commonly regulated in Δ*ugm1* and GAG interaction conditions, two of which were *chondroitin sulfate* and *dermatan sulfate degradation*, which share the proteins ganglioside GM2 activator and beta-hexosaminidase subunit. This latter is a lysosomal component previously described as an important restrictor of *Mycobacterium marinum* growth during macrophage infection [77]. This protein has also been characterized as a peptidoglycan hydrolase that exerts its mycobactericidal effect at the macrophage plasma membrane during mycobacteria-induced secretion of lysosome [77]. In addition, *A. fumigatus* induces the secretion of other lysosomal enzymes during *in vitro* interaction with epithelial cells, and the degranulation of lysosomal enzymes appears to be responsible for fungal growth inhibition and host cell damage [78]. Curiously, DAVID analysis indicated *lysosome pathway* as being modulated by GAG in HUVECs; both ganglioside GM2 activator and beta-hexosaminidase subunit are involved in this pathway.

Other coincident pathways regulated in HUVECs by both *A. fumigatus* Δ*ugm1* and GAG included *oxidative phosphorylation*, *mitochondrial dysfunction*, and *hypoxia signaling in the cardiovascular system* (Fig. 6). It is important to highlight that mitochondria play a pivotal role in endothelial cell homeostasis under normal conditions and in endothelial dysfunction in vascular diseases [79]. Moreover, oxidative stress can induce inflammatory responses by activating transcription factors, e.g., by increasing NF-κB activation [80,81,82]. DAVID analysis also corroborated the oxidative phosphorylation pathway, as shown in Fig. 7.

Furthermore, IPA analysis of HUVECs challenged with GAG indicated regulation of *integrin-like kinase* (*ILK*) *signaling pathway* (See Fig. 5 in Ref. [28]). This pathway, which is responsible for connecting integrins to the cytoskeleton at focal adhesion plaques, leading to cell survival and adhesion maintenance [83], was also identified under less stringent conditions as being regulated in HUVECs challenged with the Δ*ugm1* mutant [28]. According to QIAGEN's Ingenuity® iReport, this pathway can be activated by TNF-α and is involved in inflammation, response to wounding, tissue invasion and cytoskeleton reorganization (data not shown).

Studies regarding *Cryptococcus neoformans* interaction with endothelial cells have suggested that the pathogen can induce cytoskeleton reorganization in HUVECs and HBMECs [84,85]. It is known that the host cellular actin cytoskeleton undergoes extensive remodeling during pathogen invasion, and some studies have indicated that cofilin phosphorylation plays an important role in actin dynamics [86,87,88]. Cofilin-1 was identified in HUVEC monolayers after interaction with *C. neoformans* [84], and this protein was also identified in the present work, showing a higher abundance level in HUVECs challenged with Δ*ugm1* [28]. Curiously, the proteomics study of the HUVEC response to *C. neoformans* suggested the modulation of proteins involved in oxidative stress [84], as shown in the present study for *A. fumigatus*.

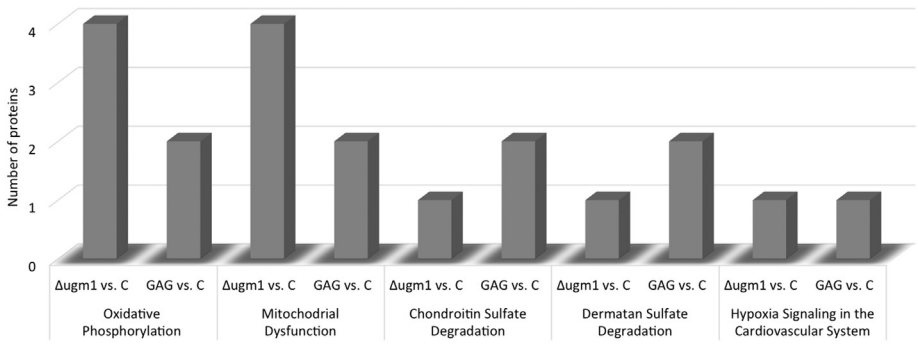

Fig. 6. Ingenuity pathway analysis showing differently regulated pathways found to be coincident between the GAG vs. control and Δ*ugm1* vs. control comparisons. The graph shows the number of proteins involved in each pathway. All of these proteins presented lower abundance levels under the interaction condition compared to the control (C). The proteins used in this analysis were filtered by cut-off values of a minimum of a 2.0 fold-change and an ANOVA *p*-value ≤ 0.05.

Please cite this article as: G.W.P. Neves, et al., Modifications to the composition of the hyphal outer layer of *Aspergillus fumigatus* modulates HUVEC proteins related to inflammatory and stress responses..., J Prot (2016), http://dx.doi.org/10.1016/j.jprot.2016.06.015

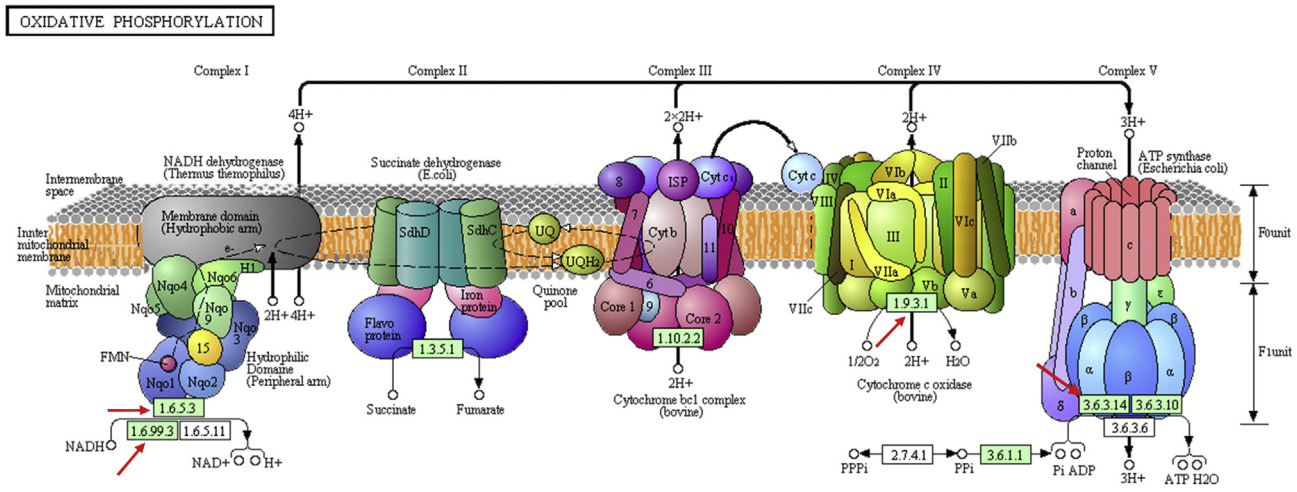

Fig. 7. Illustration of the oxidative phosphorylation pathway modulated in HUVECs challenged by the Δ*ugm1* strain. The list of proteins with differential abundance levels under the Δ*ugm1* interaction condition was analyzed by DAVID Bioinformatics Resources 6.7, and the figure was generated by the KEGG database. The red arrows indicate the genes that correspond to the proteins identified and with differential abundance levels in the Δ*ugm1* vs. control comparison.

Moreover, IPA indicated other interesting pathways related to inflammatory and stress responses as being modulated by the Δ*ugm1* strain in HUVEC monolayers (Fig. 4). Among these identified pathways, *14-3-3 signaling* is associated with apoptosis, cell cycle regulation, cellular signaling, stress and inflammatory responses (QIAGEN's Ingenuity® iReport). This pathway can respond to TNF-α and leads to Toll-like receptor (TLR) signaling via activation of the ELK-1 transcription factor (ETS domain-containing protein ELK-1) [89]. Moreover, IPA showed that *A. fumigatus* Δ*ugm1* may regulate some pathways related to antigen presentation and stress response processes, such as *protein ubiquitination* and *unfolded protein response*. In fact, endothelial cells have been described as "semiprofessional" antigen-presenting cells (APCs) because they can costimulate T cell responses *in vitro* and alloresponses *in vivo* [90,91,92,93,94]. These immune responses within blood vessels are especially important because they can lead to vascular remodeling and arteriosclerosis [95].

As mentioned above, endothelial cells are known to switch to a prothrombotic phenotype upon interaction with *A. fumigatus*, and thrombosis is a clinical feature observed in patients with invasive aspergillosis [69]. Curiously, *eNOS signaling pathway* was also highlighted by IPA as being modulated during the interaction of HUVECs with the *Δugm1* strain. eNOS, a regulator that plays a crucial role in blood vessel vasodilatation and modulates platelet aggregation, platelet and leukocyte adhesion to the endothelium, endothelin-1 generation, vascular smooth muscle proliferation and angiogenesis, is released by endothelial cells [96,97].

The role of GAG and other cell surface molecules expressed by *A. fumigatus* has remained somewhat controversial [20,21,22]. Interestingly, other molecules also present on the cell wall, such as melanin, have different effects on the host response by phagocytic and non-phagocytic cells [76]. These observations suggest that different host cell types have particular responses to the same molecule. Along these lines, our findings are in line with another recent report showing the activation of human platelets by GAG [76].

In contrast, despite fungal growth, GAG-treated mice did not exhibit inflammatory histopathology in the lung, and the cytokine expression pattern in lung homogenates showed an inhibition of protective Th1/Treg cells and a promotion of Th2 responses [22]. These anti-inflammatory effects of GAG were further related to the induction of interleukine-1 antagonist receptor [22] and also neutrophil apoptosis mediated by natural killer cells [21]. Accordingly, a murine model of invasive aspergillosis revealed that GAG was not able to confer protection against *A. fumigatus* infection [19]. However, as discussed above, the immunomodulatory role of GAG in the host remains intriguing [20,21,22].

Collectively, our results contribute new findings suggesting that the *A. fumigatus* mutant *Δugm1* and purified GAG induce a pro-inflammatory HUVEC phenotype and a cell stress response. Within this context, we hypothesize that the global GAG effect on the immune response depends on the balance between its immunosuppressive effect on neutrophils and macrophages and the activation effect observed on platelets and endothelial cells.

5. Conclusion

In conclusion, modifications to the *A. fumigatus* cell wall composition related to galactosaminogalactan (GAG) expression appear to modulate the endothelium inflammatory and cell stress responses. Our results for purified GAG suggest that this cell wall polysaccharide can modulate and activate the endothelium response to *A. fumigatus*. Other studies to confirm the role of GAG in the endothelial response during invasive aspergillosis are ongoing.

Supplementary data to this article can be found online at http://dx.doi.org/10.1016/j.jprot.2016.06.015.

Transparency document

The Transparency document associated with this article can be found, in the online version.

Acknowledgments

The authors are grateful to Glenda Sanches for her skilled technical help in preparing the primary HUVEC cultures. In addition, the authors would like to thank the RPT03C sub-unit of the PDTIS facility (Fiocruz) for access to the Luminex 200 equipment (Miliplex) and Professor Marcia Cristina Veiga Amorim for access to the scanning electronic microscope of Chemistry Institute. The authors would also like to thank the Carmela Dutra Hospital and the volunteer placenta donors who made this work possible. This work was supported by the Fundação Carlos Chagas de Amparo à Pesquisa do Estado do Rio de Janeiro (FAPERJ), grants E-26/100.329/2014 and E-26/102819/2012. LMLB is a research fellow of Conselho Nacional de Desenvolvimento Científico e Tecnológico (CNPq) and Faperj, and GWPN is a PhD Nota 10 fellow of FAPERJ.

References

[1] G.P. Bodey, S. Vartivarian, Aspergillosis, Eur. J. Clin. Microbiol. Infect. Dis. 8 (1989) 413–437.
[2] R.S. Fraser, Pulmonary aspergillosis: pathologic and pathogenetic features, Pathol. Annu. 28 (1993) 231–277.
[3] P.J. Barth, C. Rossberg, S. Koch, A. Ramaswamy, Pulmonary aspergillosis in an unselected autopsy series, Pathol. Res. Pract. 196 (2000) 73–80.
[4] D.A. Stevens, Clinical aspergillosis for basic scientists, Med. Mycol. 47 (2009) S1–S4.
[5] J.P. Latgé, *Aspergillus fumigatus* and aspergillosis, Clin. Microbiol. Rev. 12 (1999) 310–350.
[6] S.G. Filler, D.C. Sheppard, Fungal invasion of normally non-phagocytic host cells, PLoS Pathog. 2 (2006), e129.
[7] Y. Kamai, A.S. Lossinsky, H. Liu, D.C. Sheppard, S.G. Filler, Polarized response of endothelial cells to invasion by *Aspergillus fumigatus*, Cell. Microbiol. 11 (2009) 170–182.
[8] L.M. Lopes-Bezerra, S.G. Filler, Interactions of *Aspergillus fumigatus* with endothelial cells: internalization, injury, and stimulation of tissue factor activity, Blood 103 (2004) 2143–2149.
[9] L.Y. Chiang, D.C. Sheppard, F.N. Gravelat, T.F. Patterson, S.G. Filler, *Aspergillus fumigatus* stimulates leukocyte adhesion molecules and cytokine production by endothelial cells *in vitro* and during invasive pulmonary disease, Infect. Immun. 76 (2008) 3429–3438.
[10] C. Loussert, C. Schmitt, M. Prevost, V. Balloy, E. Fadel, B. Philippe, C. Kauffmann-Lacroix, J.P. Latgé, A. Beauvais, *In vivo* biofilm composition of *Aspergillus fumigatus*, Cell. Microbiol. 12 (2010) 405–410.
[11] A. Beauvais, C. Schmidt, S. Guadagnini, P. Roux, E. Perret, C. Henry, S. Paris, A. Mallet, M.C. Prévost, J.P. Latgé, An extracellular matrix glues together the aerial-grown hyphae of *Aspergillus fumigatus*, Cell. Microbiol. 9 (2007) 1588–1600.
[12] J.P. Latgé, H. Kobayashi, J.P. Debeaupuis, M. Diaquin, J. Sarfati, J.M. Wieruszeski, E. Parra, J.P. Bouchara, B. Fournet, Chemical and immunological characterization of the extracellular galactomannan of *Aspergillus fumigatus*, Infect. Immun. 62 (1994) 5424–5433.
[13] T. Fontaine, C. Simenel, G. Dubreucq, O. Adam, M. Delepierre, J. Lemoine, C.E. Vorgias, M. Diaquin, J.P. Latgé, Molecular organization of the alkali-insoluble fraction of *Aspergillus fumigatus* cell wall, J. Biol. Chem. 275 (2000) 27594–27607.
[14] L. Heesemann, A. Kotz, B. Echtenacher, M. Broniszewska, F. Routier, P. Hoffmann, F. Ebel, Studies on galactofuranose-containing glycostructures of the pathogenic mold *Aspergillus fumigatus*, Int. J. Med. Microbiol. 301 (2011) 523–530.
[15] W. Morelle, M. Bernard, J.P. Debeaupuis, M. Buitrago, M. Tabouret, J.P. Latgé, Galactomannoproteins of *Aspergillus fumigatus*, Eukaryot. Cell 4 (2005) 1308–1316.
[16] C. Costachel, B. Coddeville, J.P. Latgé, T. Fontaine, Glycosylphosphatidylinositol-anchored fungal polysaccharide in *Aspergillus fumigatus*, J. Biol. Chem. 280 (2005) 39835–39842.
[17] C. Simenel, B. Coddeville, M. Delepierre, J.P. Latgé, T. Fontaine, Glycosylinositolphosphoceramides in *Aspergillus fumigatus*, Glycobiology 18 (2008) 84–96.
[18] C. Lamarre, R. Beau, V. Balloy, T. Fontaine, J.W. Sak Hoi, S. Guadagnini, N. Berkova, M. Chignard, A. Beauvais, J.P. Latgé, Galactofuranose attenuates cellular adhesion of *Aspergillus fumigatus*, Cell. Microbiol. 11 (2009) 1612–1623.
[19] T. Fontaine, A. Delangle, C. Simenel, B. Coddeville, v.V. SJ, Y. van Kooyk, S. Bozza, S. Moretti, F. Schwarz, C. Trichot, M. Aebi, M. Delepierre, C. Elbim, L. Romani, L. JP, Galactosaminogalactan, a new immunosuppressive polysaccharide of *Aspergillus fumigatus*, PLoS Pathog. 7 (2011), e1002372.
[20] F.N. Gravelat, A. Beauvais, H. Liu, M.J. Lee, B.D. Snarr, D. Chen, W. Xu, I. Kravtsov, C.M. Hoareau, G. Vanier, M. Urb, P. Campoli, Q. Al Abdallah, M. Lehoux, J.C. Chabot, M.C. Ouimet, S.D. Baptista, J.H. Fritz, W.C. Nierman, J.P. Latgé, A.P. Mitchell, S.G. Filler, T. Fontaine, D.C. Sheppard, *Aspergillus* galactosaminogalactan mediates adherence to host constituents and conceals hyphal β-glucan from the immune system, PLoS Pathog. 9 (2013), e1003575.
[21] P. Robinet, F. Baychelier, T. Fontaine, C. Picard, P. Debre, V. Vieillard, J.P. Latgé, C. Elbim, A polysaccharide virulence factor of a human fungal pathogen induces neutrophil apoptosis via NK cells, J. Immunol. 192 (2014) 5332–5342.
[22] M.S. Gresnigt, S. Bozza, K.L. Becker, L.A. Joosten, S. Abdollahi-Roodsaz, v. der Berg WB, D. CA., N. MG, T. Fontaine, A. De Luca, S. Moretti, L. Romani, L. JP, v. de Veerdonk FL, A polysaccharide virulence factor from *Aspergillus fumigatus* elicits anti-inflammatory effects through induction of interleukin-1 receptor antagonist, PLoS Pathog. 10 (2014), e1003936.
[23] M.E. Da Silva Ferreira, M.R.V.Z. Kress, M. Savoldi, M.H.S. Goldman, A. Härtl, T. Heinekamp, A.A. Brakhage, G.H. Goldman, The akuB(KU80) mutant deficient for nonhomologous end joining is a powerful tool for analyzing pathogenicity in *Aspergillus fumigatus*, Eukaryot. Cell 5 (2006) 207–211.
[24] E. Jaffe, R.L. Nachman, C.G. Becker, C.R. Minick, Culture of human endothelial cells derived from umbilical veins. Identification by morphologic and immunologic criteria, J. Clin. Invest. 52 (1973) 2745–2756.
[25] F. Denizot, R. Lang, Rapid colorimetric assay for cell growth and survival. Modifications to the tetrazolium dye procedure giving improved sensitivity and reliability, J. Immunol. Methods 89 (1986) 271–277.
[26] C.P. Semighini, Z.P. de Camargo, R. Puccia, M.H. Goldman, G.H. Goldman, Molecular identification of *Paracoccidioides brasiliensis* by 5′ nuclease assay, Diagn. Microbiol. Infect. Dis. 44 (2002) 383–386.
[27] N. Curty, P.H. Kubitschek-Barreira, G.W. Neves, D. Gomes, L. Pizzatti, E. Abdelhay, G.H. Souza, L.M. Lopes-Bezerra, Discovering the infectome of human endothelial cells challenged with *Aspergillus fumigatus* applying a mass spectrometry label-free approach, J. Proteome 97 (2014) 126–140.
[28] G.W.P. Neves, N.A. Curty, P.H. Kubitschek-Barreira, T. Fontaine, G.H. Souza, M.L. Cunha, G.H. Goldman, A. Beauvais, J.P. Latgé, L.M. Lopes-Bezerra, Proteomic profiling of HUVECs challenged with wild type and *UGM1* mutant *Aspergillus fumigatus* strains, Data in Brief (2016).
[29] J.C. Silva, R. Denny, C.A. Dorschel, M. Gorenstein, I.J. Kass, G.Z. Li, T. McKenna, M.J. Nold, K. Richardson, P. Young, S. Geromanos, Quantitative proteomic analysis by accurate mass retention time pairs, Anal. Chem. 77 (2005) 2187–2200.
[30] J.C. Silva, G. M.V., G. Li, J.P.C. Vissers, S.J. Geromanos, Absolute quantification of proteins by LCMS^{E}. A virtue of parallel MS acquisition, Mol. Cell. Proteomics 5 (2006) 144–156.
[31] G.Z. Li, J.P. Vissers, J.C. Silva, D. Golick, M.V. Gorenstein, S.J. Geromanos, Database searching and accounting of multiplexed precursor and product ion spectra from the data independent analysis of simple and complex peptide mixtures, Proteomics 9 (2009) 1696–1719.
[32] The UniProt Consortium, UniProt: a hub for protein information, Nucleic Acids Res. 43 (2015) D204–D212.
[33] V.B. Abdul-Salam, J. Wharton, J. Cupitt, M. Berryman, R.J. Edwards, M.R. Wilkins, Proteomic analysis of lung tissues from patients with pulmonary arterial hypertension, Circulation 122 (2010) 2058–2067.
[34] M. Affolter, L. Grass, F. Vanrobaeys, B. Casado, M. Kussmann, Qualitative and quantitative profiling of the bovine milk fat globule membrane proteome, J. Proteome 73 (2010) 1079–1088.
[35] L. Dicker, X. Lin, A.R. Ivanov, Increased power for the analysis of label-free LC-MS/MS proteomics data by combining spectral counts and peptide peak attributes, Mol. Cell. Proteomics 9 (2010) 2704–2718.
[36] S.M. Hauck, J. Dietter, R.L. Kramer, F. Hofmaier, J.K. Zipplies, B. Amann, A. Feuchtinger, C.A. Deeg, M. Ueffing, Deciphering membrane-associated molecular processes in target tissue of autoimmune uveitis by label-free quantitative mass spectrometry, Mol. Cell. Proteomics 9 (2010) 2292–2305.
[37] Y. Levin, S. Bahn, Quantification of proteins by label-free LC-MS/MS, Methods Mol. Biol. 658 (2010) 217–231.
[38] R. Zhang, A. Barton, J. Brittenden, J.T.J. Huang, D. Crowther, Evaluation for computational platforms of LC-MS based label-free quantitative proteomics: a global view, J. Proteomics Bioinform. 3 (2010) 260–265.
[39] Y. Levin, The role of statistical power analysis in quantitative proteomics, Proteomics 11 (2011) 2565–2567.
[40] K.A. Neilson, N.A. Ali, S. Muralidharan, M. Mirzaei, M. Mariani, G. Assadourian, A. Lee, S.C. van Sluyter, P.A. Haynes, Less label, more free: approaches in label-free quantitative mass spectrometry, Proteomics 11 (2011) 535–553.
[41] M. Sandin, M. Krogh, K. Hansson, F. Levander, Generic workflow for quality assessment of quantitative label-free LC-MS analysis, Proteomics 11 (2011) 1114–1124.
[42] K. Wada, A. Ogiwara, K. Nagasaka, N. Tanaka, Y. Komatsu, i-RUBY: a novel software for quantitative analysis of highly accurate shotgun-proteomics liquid chromatography/tandem mass spectrometry data obtained without stable-isotope labeling of proteins, Rapid Commun. Mass Spectrom. 25 (2011) 960–968.
[43] C.M. Colangelo, M. Shifman, K.H. Cheung, K.L. Stone, N.J. Carriero, E.E. Gulcicek, T.T. Lam, T. Wu, R.D. Bjornson, C. Bruce, A.C. Nairn, J. Rinehart, P.L. Miller, K.R. Williams, YPED: an integrated bioinformatics suite and database for mass spectrometry-based proteomics research, Genomics Proteomics Bioinformatics 13 (2015) 25–35.
[44] E. Oveland, T. Muth, E. Rapp, L. Martens, F.S. Berven, H. Barsnes, Viewing the proteome: how to visualize proteomics data? Proteomics 15 (2015) 1341–1355.
[45] L.M. Brown, Quantitative shotgun proteomics with data-independent acquisition and traveling wave ion mobility spectrometry: a versatile tool in the life sciences, Adv. Exp. Med. Biol. 806 (2014) 79–91.
[46] A. Chawade, M. Sandin, J. Teleman, J. Malmstrom, F. Levander, Data processing has major impact on the outcome of quantitative label-free LC-MS analysis, J. Proteome Res. 14 (2014) 676–687.
[47] M. Choi, C.Y. Chang, T. Clough, D. Broudy, T. Killeen, B. MacLean, O. Vitek, MSstats: an R package for statistical analysis of quantitative mass spectrometry-based proteomic experiments, Bioinformatics 30 (2014) 2524–2526.
[48] S. Gerster, T. Kwon, C. Ludwig, M. Matondo, C. Vogel, E.M. Marcotte, R. Aebersold, P. Buhlmann, Statistical approach to protein quantification, Mol. Cell. Proteomics 13 (2014) 666–677.
[49] S.W. Haga, H.F. Wu, Overview of software options for processing, analysis and interpretation of mass spectrometric proteomic data, J. Mass Spectrom. 49 (2014) 959–969.
[50] D. Helm, J.P. Vissers, C.J. Hughes, H. Hahne, B. Ruprecht, F. Pachl, A. Grzyb, K. Richardson, J. Wildgoose, S.K. Maier, H. Marx, M. Wilhelm, I. Becher, S. Lemeer, M. Bantscheff, J.I. Langridge, B. Kuster, Ion mobility tandem mass spectrometry enhances performance of bottom-up proteomics, Mol. Cell. Proteomics 13 (2014) 3709–3715.
[51] T. Wilhelm, A.M. Jones, Identification of related peptides through the analysis of fragment ion mass shifts, J. Proteome Res. 13 (2014) 4002–4011.
[52] N.J. Bond, P.V. Shliaha, K.S. Lilley, L. Gatto, Improving qualitative and quantitative performance for MS(E)-based label-free proteomics, J. Proteome Res. 12 (2013) 2340–2353.
[53] S. Nahnsen, C. Bielow, K. Reinert, O. Kohlbacher, Tools for label-free peptide quantification, Mol. Cell. Proteomics 12 (2013) 549–556.
[54] E. Rodriguez-Suarez, A.D. Whetton, The application of quantification techniques in proteomics for biomedical research, Mass Spectrom. Rev. 32 (2013) 1–26.
[55] H. Weisser, S. Nahnsen, J. Grossmann, L. Nilse, A. Quandt, H. Brauer, M. Sturm, E. Kenar, O. Kohlbacher, R. Aebersold, L. Malmstrom, An automated pipeline for high-throughput label-free quantitative proteomics, J. Proteome Res. 12 (2013) 1628–1644.
[56] M. Bantscheff, S. Lemeer, M.M. Savitski, B. Kuster, Quantitative mass spectrometry in proteomics: critical review update from 2007 to the present, Anal. Bioanal. Chem. 404 (2012) 939–965.
[57] S. Lemeer, H. Hahne, F. Pachl, B. Kuster, Software tools for MS-based quantitative proteomics: a brief overview, Methods Mol. Biol. 893 (2012) 489–499.

Please cite this article as: G.W.P. Neves, et al., Modifications to the composition of the hyphal outer layer of *Aspergillus fumigatus* modulates HUVEC proteins related to inflammatory and stress responses..., J Prot (2016), http://dx.doi.org/10.1016/j.jprot.2016.06.015

[58] D. Qi, P. Brownridge, D. Xia, K. Mackay, F.F. Gonzalez-Galarza, J. Kenyani, V. Harman, R.J. Beynon, A.R. Jones, A software toolkit and interface for performing stable isotope labeling and top3 quantification using Progenesis LC-MS, OMICS 16 (2012) 489–495.

[59] D.W. Huang, S. B.T., R.A. Lempicki, Systematic and integrative analysis of large gene lists using DAVID bioinformatics resources, Nat. Protoc. 4 (2008) 44–57.

[60] J.A. Vizcaíno, E.W. Deutsch, R. Wang, A. Csordas, F. Reisinger, D. Ríos, J.A. Dianes, Z. Sun, T. Farrah, N. Bandeira, P.A. Binz, I. Xenarios, M. Eisenacher, G. Mayer, L. Gatto, A. Campos, R.J. Chalkley, H.J. Kraus, J.P. Albar, S. Martinez-Bartolomé, R. Apweiler, G.S. Omenn, L. Martens, A.R. Jones, H. Hermjakob, ProteomeXchange provides globally coordinated proteomics data submission and dissemination, Nat. Biotechnol. 32 (2014) 223–226.

[61] J.A. Vizcaíno, R.G. Cote, A. Csordas, J.A. Dianes, A. Fabregat, J.M. Foster, J. Griss, E. Alpi, M. Birim, J. Contell, G. O'Kelly, A. Schoenegger, D. Ovelleiro, Y. Perez-Riverol, F. Reisinger, D. Rios, R. Wang, H. Hermjakob, The proteomics identifications (PRIDE) database and associated tools: status in 2013, Nucleic Acids Res. 41 (D1) (2013) D1063–D1069.

[62] K. Seidl, N.V. Solis, A.S. Bayer, W.A. Hady, S. Ellison, M.C. Klashman, Y.Q. Xiong, FillerSG.Divergent responses of different endothelial cell types to infection with *Candida albicans* and *Staphylococcus aureus*, PLoS ONE 7 (6) (2012) 39633.

[63] N.A. Karp, M. Spencer, H. Lindsay, K. O'Dell, K.S. Lilley, Impact of replicate types on proteomic expression analysis, J. Proteome Res. 4 (5) (2005) 1867–1871.

[64] D. Wang, J. Feng, R. Wen, J.C. Marine, M.Y. Sangster, E. Parganas, et al., Phospholipase Cg2 is essential in the functions of B cell and several Fc receptors, Immunity 13 (1) (2000) 25–35.

[65] Z. Li, M.K. Delaney, K.A. O'Brien, X. Du, Signaling during platelet adhesion and activation, Arterioscler. Thromb. Vasc. Biol. 30 (12) (2010) 2341–2349.

[66] P.M. Kloetzel, Antigen processing by the proteasome, Nat. Rev. Mol. Cell Biol. 2 (2001) 179–188.

[67] D. Zuo, J. Subjeck, Wang XYUnfolding the role of large heat shock proteins: new insights and therapeutic implications, Front. Immunol. 7 (2016) 75.

[68] Q. Wan, E. Kuang, W. Dong, S. Zhou, H. Xu, Y. Qi, Y. Liu, Reticulon 3 mediates Bcl-2 accumulation in mitochondria in response to endoplasmic reticulum stress, Apoptosis 12 (2) (2007) 319–328.

[69] A. Warris, The biology of pulmonary *aspergillus* infections, J. Infect. 69 (2014) S36–S41.

[70] L.M. Lopes-Bezerra, S.G. Filler, Endothelial cells, tissue factor and infectious diseases, Braz. J. Med. Biol. Res. 36 (8) (2003) 987–991.

[71] D.C. Sheppard, Molecular mechanism of *Aspergillus fumigatus* adherence to host constituents, Curr. Opin. Microbiol. 14 (2011) 375–379.

[72] D.C. Sheppard, S.G. Filler, Host cell invasion by medically important fungi, Cold Spring Harb. Perspect. Med. 5 (1) (2014) a019687.

[73] J.P. Latgé, Tasting the fungal cell wall, Cell. Microbiol. 12 (2010) 863–872.

[74] A. Beauvais, T. Fontaine, V. Aimanianda, J.P. Latgé, *Aspergillus* cell wall and biofilm, Mycopathologia 178 (2014) 371–377.

[75] M.J. Lee, F.N. Gravelat, R.P. Cerone, S.D. Baptista, P.V. Campoli, S.I. Choe, I. Kravtsov, E. Vinogradov, C. Creuzenet, H. Liu, A.M. Berghuis, J.P. Latgé, S.G. Filler, T. Fontaine, D.C. Sheppard, Overlapping and distinct roles of *Aspergillus fumigatus* UDP-glucose 4-epimerases in galactose metabolism and the synthesis of galactose-containing cell wall polysaccharides, J. Biol. Chem. 289 (2014) 1243–1256.

[76] G. Rambach, G. Blum, J.P. Latgé, T. Fontaine, T. Heinekamp, M. Hagleitner, H. Jeckström, G. Weigel, P. Würtinger, K. Pfaller, S. Krappmann, J. Löffler, C. Lass-Flörl, C. Speth, Identification of *Aspergillus fumigatus* surface components that mediate interaction of conidia and hyphae with human platelets, J. Infect. Dis. 212 (2015) 1140–1149.

[77] I.C. Koo, Y.M. Ohol, P. Wu, J.H. Morisaki, J.S. Cox, E.J. Brown, Role for lysosomal enzyme beta-hexosaminidase in the control of mycobacteria infection, Proc. Natl. Acad. Sci. U. S. A. 105 (2) (2008) 710–715.

[78] A. Fekkar, V. Balloy, C. Pionneau, C. Marinach-Patrice, M. Chignard, D. Mazier, Secretome of human bronchial epithelial cells in response to the fungal pathogen *Aspergillus fumigatus* analyzed by differential in-gel electrophoresis, J. Infect. Dis. 205 (7) (2012) 1163–1172.

[79] X. Tang, Y. Luo, H. Chen, D. Liu, Mitochondria, endothelial cell function, and vascular diseases, Front. Physiol. 5 (2014) 175.

[80] F. Arnalich, E. Garcia-Palomero, J. Lopez, Predictive value of NFkB activity and plasma cytokine levels in patients with sepsis, Infect. Immun. 68 (2000) 1942–1945.

[81] R.L. Paterson, H.F. Galley, J.K. Dhillon, N.R. Webster, Increased NFkB activation in critically ill patients who die, Crit. Care Med. 28 (2000) 1047–1051.

[82] A.L. Hill, D.A. Lowes, N.R. Webster, C.C. Sheth, N.A. Gow, H.F. Galley, Regulation of pentraxin-3 by antioxidants, Br. J. Anaesth. 103 (2009) 833–839.

[83] S.H. Lo, Focal adhesions: what's new inside, Dev. Biol. 294 (2) (2006) 280–291.

[84] X.J. Wang, Y.J. Zhu, J.G. Cui, X. Huang, J. Gu, H. Xu, H. Wen, Proteomic analysis of human umbilical vein endothelial cells incubated with *Cryptococcus neoformans var. neoformans*, Mycoses 54 (5) (2011) e336–e343.

[85] S.H. Chen, M.F. Stins, S.H. Huang, Y.H. Chen, K.J. Kwon-Chung, Y. Chang, K.S. Kim, K. Suzuki, A.Y. Jong, *Cryptococcus neoformans* induces alterations in the cytoskeleton of human brain microvascular endothelial cells, J. Med. Microbiol. 52 (Pt11) (2003) 961–970.

[86] E. Euge'ne, I. Hoffmann, C. Pujol, C. PO, S. Bourdoulous, X. Nassif, Microvilli-like structures are associated with the internalization of virulent capsulated Neisseria meningitidis into vascular endothelial cells, J. Cell Sci. 115 (2002) 1231–1241.

[87] H. Bierne, E. Gouin, P. Roux, P. Caroni, H.L. Yin, P. Cossart, A role for cofilin and LIM kinase in Listeria-induced phagocytosis, J. Cell Biol. 155 (2001) 101–112.

[88] R. Niwa, K. Nagata-Ohashi, M. Takeichi, K. Mizuno, T. Uemura, Control of actin reorganization by Slingshot, a family of phosphatases that dephosphorylate ADF/cofilin, Cell 108 (2002) 233–246.

[89] T. Kawai, S. Akira, The role of pattern-recognition receptors in innate immunity: update on Toll-like receptors, Nat. Immunol. 11 (2010) 373–384.

[90] T. Geppert, P. Lipsky, Antigen presentation by interferon-gamma-treated endothelial cells and fibroblasts: differential ability to function as antigen-presenting cells despite comparable Ia expression, J. Immunol. 135 (1985) 3750–3762.

[91] H. Kosaka, C.D. Surh, J. Sprent, Stimulation of mature unprimed CD8+ T cells by semiprofessional antigen-presenting cells in vivo, J. Exp. Med. 176 (1992) 1291–1302.

[92] M. Vora, H. Yssel, J. de Vries, M. Karasek, Antigen presentation by human dermal microvascular endothelial cells. Immunoregulatory effect of IFN-γ and IL-10, J. Immunol. 152 (1994) 5734–5741.

[93] D.M. Briscoe, L.E. Henault, C. Geehan, S.I. Alexander, A.H. Lichtman, Human endothelial cell costimulation of T cell IFN-gamma production, J. Immunol. 159 (1997) 3247–3256.

[94] F.M. Marelli-Berg, D. Scott, I. Bartok, E. Peek, J. Dyson, R.I. Lechler, Activated murine endothelial cells have reduced immunogenicity for CD8+ T cells: a mechanism of immunoregulation? J. Immunol. 165 (2000) 4182–4189.

[95] R. Ross, Atherosclerosis — an inflammatory disease, N. Engl. J. Med. 340 (1999) 115–126.

[96] F.M. Ho, W.W. Lin, B.C. Chen, C.M. Chao, C.R. Yang, L.Y. Lin, C.C. Lai, S.H. Liu, C.S. Liau, High glucose-induced apoptosis in human cascular endothelial cells is mediated through NF-kappaB and c-Jun NH(2)-terminal kinase pathway and prevented by PI3K/Akt/eNOS pathway, Cell. Signal. 18 (3) (2005) 391–399.

[97] Y.C. Boo, H. Jo, Flow-dependent regulation of endothelial nitric oxide synthase: role of protein kinases, Am. J. Physiol. Cell Physiol. 285 (3) (2003) C499–C508.

Please cite this article as: G.W.P. Neves, et al., Modifications to the composition of the hyphal outer layer of *Aspergillus fumigatus* modulates HUVEC proteins related to inflammatory and stress responses..., J Prot (2016), http://dx.doi.org/10.1016/j.jprot.2016.06.015